



Toward accurate olefin quantification in plastic waste oils: Analytical strategies and future directions

Miloš Auersvald^{a,b,*}, Genesis Barzallo^{c,d,e}, Hung Gieng^c, Jyotika Patel^c, Ananya Sharma^c, Kevin M. Van Geem^b, Petr Straka^a, Petr Vozka^{c,**}

^a Department of Sustainable Fuels and Green Chemistry, University of Chemistry and Technology Prague, Technická 5, 166 28 Prague 6, Czech Republic

^b Ghent University, Laboratory for Chemical Technology, Technologiepark 125, 9052, Ghent, Belgium

^c Department of Chemistry and Biochemistry, California State University, Los Angeles, 5151 State University Dr., Los Angeles, CA, 90032, USA

^d Herbert Wertheim School of Public Health, University of California San Diego, San Diego, CA, 92093, USA

^e School of Public Health, San Diego State University, San Diego, CA, 92182, USA

ARTICLE INFO

Keywords:

Olefin
Quantification
Pyrolysis
Hydrothermal liquefaction
Plastic
Chromatography

ABSTRACT

The global production of plastic waste exceeds 400 million tons annually, driving interest in chemical recycling processes like pyrolysis and hydrothermal liquefaction. These technologies generate hydrocarbon-rich oils with high olefin content, offering valorization opportunities but also presenting challenges for storage stability and upgrading. Accurate quantification of olefins in these complex mixtures remains a major analytical bottleneck. This review critically examines established and emerging methods for olefin analysis, including titration, FTIR and NMR spectroscopy, chromatographic approaches (1D-GC, GC × GC, HPLC), and selective strategies such as silver-ion complexation, chemical derivatization, and low-energy ionization mass spectrometry. We emphasize the limitations of standardized techniques and the potential of advanced approaches, particularly GC × GC-VUV and soft ionization MS, for enhanced selectivity and sensitivity. Finally, we highlight persistent gaps in method validation, standardization, and isomer discrimination, and propose research directions to improve analytical accuracy, reproducibility, and applicability to the complex matrices found in plastic-derived oils.

1. Introduction

Global plastic production surpasses 400 million tons annually, with polyolefins (PE, PP) accounting for ~57 % of the output and 63 % of the landfilled plastic waste [1]. Cumulatively, ~6 billion tons of plastic reside in landfills and oceans; only ~9 % is recycled and ~12 % incinerated [2]. [3]. Thermochemical processes (pyrolysis and hydrothermal processing) convert polyolefin wastes into oil-like products by cleaving long chains into shorter oligomers, generating short-lived free radicals and alkenes.

Olefin content is tightly regulated in gasoline fuel: ≤18 vol% (EN 228, Europe), 10 vol% (EPA, USA), and 6 vol% (CARB, California). These regional limits reflect differences in ozone-attainment status, fuel-specification history, region-specific refinery configurations, and vehicle-fleet characteristics. California's stricter 6 vol% cap is driven by its more ambitious air-quality objectives and the basin meteorology that

amplifies ozone formation.

Compared with petroleum fractions, plastic-derived oils (POs) typically contain significantly higher concentrations of olefins, which drive thermo-oxidative instability during storage [4] and increase coke formation/fouling during steam cracking to light olefins [5]. POs also carry higher contaminant levels (N, S, O, halogens, trace metals), causing corrosion and catalyst poisoning. Hydrogenation-based upgrading is often necessary to meet industrial feedstock specifications, yet feedstock quality remains variable due to consumer behavior, seasonal variations, and local sorting efficiencies [5].

As olefins are a major functional group in POs, their accurate identification and quantification are critical for advancing PO valorization. Currently, most studies rely on analytical methods developed for petroleum products, often without validating their suitability or recognizing their limitations. This can lead to misinterpretation of olefin content and reduce the comparability of results across studies. This

* Corresponding author. Department of Sustainable Fuels and Green Chemistry, University of Chemistry and Technology Prague, Technická 5, 166 28 Prague 6, Czech Republic.

** Corresponding author.

E-mail addresses: milos.auersvald@vscht.cz (M. Auersvald), pvozka@calstatela.edu (P. Vozka).

<https://doi.org/10.1016/j.trac.2025.118463>

Received 20 June 2025; Received in revised form 11 September 2025; Accepted 14 September 2025

Available online 19 September 2025

0165-9936/© 2025 The Authors. Published by Elsevier B.V. This is an open access article under the CC BY license (<http://creativecommons.org/licenses/by/4.0/>).

review aims to support researchers working on plastic chemical recycling via thermochemical processes in selecting the most reliable methods for determining olefins in pyrolysis oils.

Olefin analysis in cracked petroleum streams has been reviewed extensively (e.g., Badoni et al., 1992) [6] across various chemical and instrumental methods and relevant ASTM/IP/UOP procedures [6]. While capillary gas chromatography (GC) is reliable up to 100 °C, higher boiling fractions demand hyphenated or selected workflows (HPLC-GC, GC-MS, HPLC-MS), and isomer-level identification remains challenging. Conjugated diene determination has likewise been surveyed (Andrade et al., 2010) [7], with voltammetry enabling rapid total dienes and GC and NMR offering greater specificity at higher method complexity [7]. For plastic-derived oils specifically, recent work emphasizes molecular-level characterization by GC × GC; the first PO application was reported by Toraman et al. (2014) and was synthesized by Zanella et al. (2023) [8] [9], marking a significant milestone in the field.

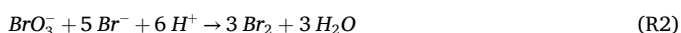
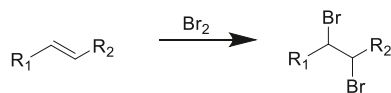
This review (1995–2025) focuses explicitly on **quantifying olefins in plastic-derived oils**. To our knowledge, no prior literature review has focused on this topic. This review explores various analytical methods, including **titration** (bromine, iodine), **spectroscopic** (FTIR, NMR), and **chromatographic** (liquid, gas) **techniques**, as well as **selective approaches** such as **low-energy ionization**, **derivatization**, and **adsorption methods**. Across the following subsections, we examine methods for olefin determination (qualitative and quantitative), organized by analytical instrument family or approach, and highlight their advantages, limitations, and distinguishing features. For each method, we summarize application range, potential interferences, and accuracy/LOD considerations and outline practical implementation, integrating literature benchmarks with our measurements on model compounds and diverse plastic-pyrolysis samples (our experience indicated in *italics*). Key information and section summaries are highlighted in **bold**. A brief overview of possible methods, including key information, is summarized in Table 1, which can also serve as a table of contents.

2. Titration methods

Total olefin content in plastic pyrolysis oils is most commonly measured by halogen-addition titrations: Bromine number (Section 2.1), Bromine index (Section 2.2), and Iodine value (Section 2.3). These simple and cost-effective methods yield a single bulk-unsaturation result typically reported as grams of halogen per 100 g sample (convertible to mmol of C=C per gram of sample) [11]. *To our knowledge, a recent experimental study [16] compared these titrations, validating their suitability for POs.*

2.1. Bromine number (BrN)

BrN quantifies bulk olefin unsaturation via **electrophilic addition** (R1) of bromine to the C=C bond (ASTM D1159), originating from the Dubois and Skoog titration [11]. In practice, Br₂ is generated in situ from KBr–KBrO₃ (R2) in acid, the sample is dissolved in a solvent mixture of acetic acid (71.4 vol%), dichloromethane (13.4 vol%), methanol (13.4 vol%), and sulfuric acid (1.8 vol%; 16.6 % conc.). *Although the direct weighing of the sample into the titration beaker or cup seems the most convenient approach, dissolving the sample in a suitable solvent, such as dichloromethane or toluene, as suggested by the ASTM standard, could help eliminate problems with sample solubility typical for POs from polyolefin-rich waste.*



The endpoint is determined electrometrically at 0–5 °C to suppress substitution reactions and minimize losses of light olefins [11]. Results are reported as g Br₂ per 100 g of a sample and can be converted to mmol of C=C per gram for cross-method comparison. This method, primarily used for characterizing hydrocarbon samples such as fossil gasoline, could thus be considered suitable for quantifying olefins in POs.

Several limitations have been identified in characterizing POs based on the ASTM D1159 standard and its annexes, particularly Annex A1, which details the reactivity of numerous model compounds. This method under-responds to linear α-olefins, common in PE-derived oils [12] and reacts with only one double bond in conjugated dienes, biasing totals low. Typically, less than 90 % of double bonds in α-olefins can be determined [2]. ASTM D1159 is intended for samples with 90 % distillation below ~327 °C; a constraint often limiting most POs [12]. *Above this cut point, solubility at 0–5 °C becomes problematic (e.g., 1-nonadecene: b.p. 329 °C; m.p. 23 °C), and highly condensed aromatics (e.g., anthracene, b.p. 340 °C), as well as other interferents, can undergo partial substitution with Br₂, inflating results even at low temperature [12].* Interfering species (phenols, thiophenes, thiols, polyaromatics) tend to undergo substitution reactions with Br₂ and inflate apparent unsaturation [12–15]. A recent study on heteroatom-rich tire oil [16] confirmed that such side reactions were the primary source of overestimation and that larger sample sizes increased BrN via longer titration times [16]. Sulfur- and nitrogen-selective detector studies indicate thiols and thiophenes are the dominant contributors among these species in typical PO matrices, whereas pyrroles are usually minor. Nevertheless, typical sulfur levels in POs from polyolefin-rich waste are often in the hundreds of ppm, which alone should not dominate the bias [9,17]. Finally, branched olefins, prevalent in PP-rich oils, are prone to substitution at ambient temperature (as noted by Dubois and Skoog for diisobutene), further inflating BrN values [11]. *Collectively, these effects limit BrN as an absolute measure of total olefin unsaturation in POs.*

Despite these limitations, BrN is widely applied to characterize waste-plastic pyrolysis POs. Fraczak et al. [18] pyrolyzed virgin PE, PP, and PS, as well as their mixtures (spiked with PET and PVC), in a 2 kg/h pilot unit. PE-rich oils exhibited a BrN of 34.2 g Br₂/100 g. In contrast, PP-rich oils showed a significantly higher BrN of 72.8 g Br₂/100 g, consistent with prior reports [19,20] and with trends from alternative olefin metrics [21–23]. *Since BrN reflects mmol of C=C per mass, heavier (higher-boiling) fractions exhibit lower BrN; conversely, BrN increases as average boiling point decreases.* Ondrovič et al. [20] observed the same inverse relationship for PP-derived oils. Mlynková et al. [19] reported BrN of ~80 (PE) and ~100 (PP) for the naphtha cut, dropping to 50 (PE) and 80 (PP) for the diesel fraction, and hydro-treating over Pt/C catalyst reduced BrN to ~1 g Br₂/100 g [19]. For sorted waste, Gala et al. [24] found lower BrN values: 40 g Br₂/100 g for industrial and manually sorted colored plastic waste and 31 g Br₂/100 g for manually sorted white plastic waste. The PE-rich composition aligns with Fraczak et al. [18]. Dunkle et al. [25] reported a linear BrN and GC-VUV correlation, *but deviations from ASTM D1159 (titration conducted at room temperature instead of the recommended range of 0–5 °C) limit confidence; see section 6.1.*

Auersvald et al. [16] showed that ASTM D1159 cannot accurately determine the total unsaturation of pyrolysis oils from polyolefins and tires (Fig. 1). This conclusion was drawn based on (i) model compounds, (ii) olefin-free fossil kerosene spiked with an olefin mixture, and (iii) real waste-plastic and tire oils with cuts and hydrotreated products. Relative to olefin-selective GC × GC (adsorption-based) [10], BrN yielded ~40 % fewer double bonds, and most model olefins reacted >5 % below theoretical.

To conclude, BrN is not an ideal for quantifying the total unsaturation of POs. However, it is still useful for comparing reactive double-bond content across samples with similar boiling point ranges and heteroatom levels. Adjusting the sample size to achieve comparable titrant consumption can improve result comparability when interferences are expected.

Table 1

Table of contents and overview of reviewed methods for olefin quantification in plastic-waste-derived oils (POs): application range, advantages, and limitations (*when combined with GC × GC-FID as described in Ref. [10]; **when NMR end used).

Section/Method		Application range and standard method	Result/value	Advantages	Limitations
2. Titrations	2.1. BrN	Light/middle distillates (b.p.≤327 °C); ASTM D1159	Total content aliphatic = i.e. mol/g	Simple, standardized, widely used	Poor accuracy; solubility/interference issues; under/overestimation
	2.2. BrIn	Hydroprocessed - low olefin content; ASTM D2710	BrN g Br ₂ /100g BrIn mg Br/100g	Sensitive to residual unsaturation; useful for hydrotreating studies	Not suitable for crude oils; small sample sizes; solubility issues
	2.3. IV	Suitable for polyolefin-rich oils; ASTM D5554, EN 14111	IV g l/100g	Good response to linear olefins; avoids BrN solubility issues; matches GC × GC with Hg cat.	Slower, toxic reagents (ICl, Hg); polyaromatics/heteroatoms interfere; low sensitivity ≈1 %
3. Spectroscopy	3.1. FTIR	Rapid screening of olefinic structures	Relative abundance %	Fast, low-cost, clear functional-group fingerprints	Only semiquantitative; low structural detail; needs a complementary method
	3.2. Raman	Qualitative/semi-quantitative olefin detection; potential for online monitoring		Strong olefinic fingerprints; non-destructive; minimal sample prep; fiber-probe compatible	Cross-section variability; matrix effects; calibration needed for quantitation
	3.3. ¹ H NMR	Quantifies olefinic hydrogens (4.0–6.6 ppm)	Content of olefinic H mol%	Direct, selective, quantitative; whole-sample analysis; less interference vs. IR/titration	Measures H-types - not molecules; bad sensitivity; long runs/advanced methods needed
4. Liquid Chrom.	4.1. FIA	Light/mid distillates (b.p. ≤315 °C) ASTM D1319	Total content vol%	Standardized, direct vol% of olefins; comparable to GC × GC-FID for mono-olefins	Slow; LOD ~1 vol%; misclassifies dienes as aromatics
	4.2. HPLC	Group-type analysis (saturates, olefins, dienes, aromatics) in gasoline–mid distillates	Total content + per group wt% or vol%	High selectivity; low LODs; flexible with detector choice (RI, UV, ELSD)	Costly; accuracy drops <10 % olefins; careful column/detector selection required
	4.3. SFC	Olefin quantification in full-range (1–25 wt%), ASTM D6550	Total content + per group wt% or vol%	Fast, group-type; fingerprints PE vs. PP oils	Column deactivation (sulfur); no structural detail; needs MS for speciation
5. Gas Chromatography	5.1.1. 1D-GC - gases	C1–C6 olefins in pyrolysis gases, ASTM D2163, UOP 539	Individual + group content wt %	Standardized, accurate, fast; online monitoring with IS	Specialized RGA setup; calibration essential; costly
	5.1.2. 1D-GC - liquids	Naphtha-range POs (≤C10), ASTM D6729, D6733; catalytic pyrolysis; PONA/GC-MS/FID	Individual + group content wt %	Standardized DHA; compound ID with GC-MS/FID; useable with long columns	Peak co-elution; poor resolution for C8+ olefins; MS TIC area%≠wt%; RRFs use required for FID
	5.2. GC × GC	Detailed analysis; most of the sample, hydrocarbons (C3–C75+)	Individual + group content wt %	High resolution; broad separation; robust quantification with FID + MS	Labor-intensive; costly; still limited in olefin vs. naphthene separation, PTV inlet needed for heavier cuts
6. Selective methods	6.1. GC-VUV	Group-type quantification/isomer-specific; ASTM D8519 for POs	Individual + group content wt %	Distinguishes olefins/naphthenes/dienes; calibration-free analysis	Small spectral library; lower sensitivity (≈0.1 %)/dynamic range; heteroatom issues
	6.2. Soft Ionization MS	Olefin isomers/double-bond position	Relative abundance %	Intense molecular ions; diagnostic fragments; better than EI-MS	Specialized, pricy instruments (ion source PI, FI, CI); limited libraries; not standardized; cold-EI untested
	6.3. Derivatizations	Enhance separation or MS detection of olefins in complex mixtures	Relative abundance % to Individual + group content wt %	Provides double-bond position/branching info; diagnostic fragmentation	Extra prep; toxic reagents; complex spectra for polyenes, labor-intensive
	6.4. Ag ⁺ Complexations	Olefin/paraffin separation, distillates, and heavy PO cuts	Individual + group content wt %*/mol%**	Highly selective; SPE is low-cost, robust, and fast sample prep; aids GC/NMR end method	Ag ⁺ unstable (light, H ₂ S, etc.); short LC column lifetimes; structure-dependent selectivity

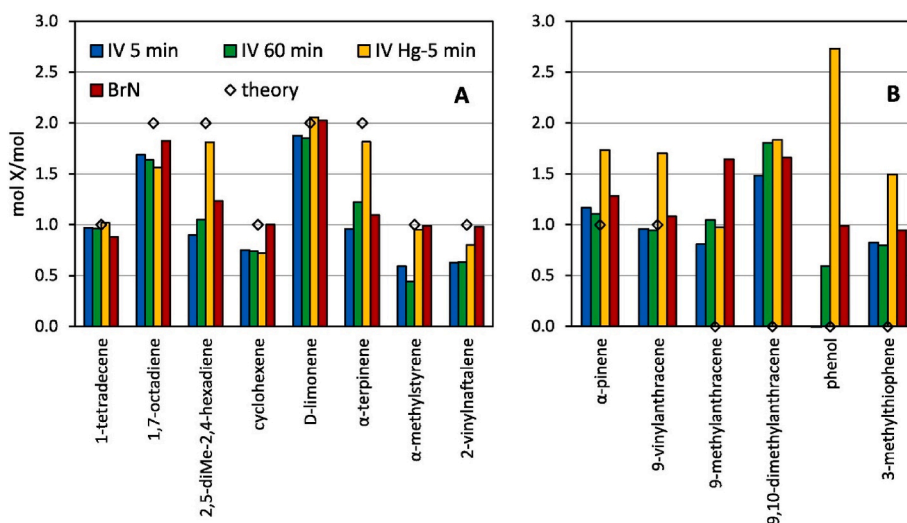


Fig. 1. Reactivity of chosen model compounds, i.e., the number of halogens (X) in mols/mol of compound theoretically reactive with all olefinic double bonds. “Typical” olefins for PO (A), “problematic” compounds in PO (B). Three IV methods differ in reaction time before titration (5 or 60 min, the latter corresponding to the standard method). The IV Hg-5min uses a Mercury (II) acetate catalyst. Reprinted with permission from Ref. [16] Copyright 2025 Elsevier.

2.2. Bromine index (BrIn)

BrIn follows the same principle as BrN, addition of bromine to the C=C (R1), but targets lower olefin contents. Results are reported in mg Br per 100 g sample (mg Br/100 g) rather than g Br₂/100 g [26,27]. Theoretically, BrIn is twice the BrN for the same sample. Two ASTM methods exist for determining the BrIn: ASTM D1492 and D2710.

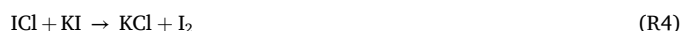
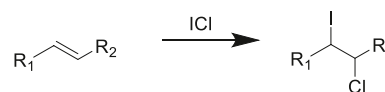
ASTM D2710 [27] closely mirrors D1159, as both are electrometric titrations, but uses a tenfold-diluted titrant (0.025 M KBr–KBrO₃). This method applies to samples with BrIn lower than 1000 mg Br/100 g. ASTM D1492 [26] is an amperometric-coulometric titration (analogous in concept to Karl Fischer titration for water determination). Br₂ is generated in situ from an electrolyte of 60 vol% acetic acid, 26 vol% methanol, and 14 vol% KBr solution (119 g/L). This method is suitable for up to 100 mg Br/100 g, i.e., even lower unsaturation than D2710. A third method, ASTM D1491 (potentiometric), was withdrawn in 1985. Since we could not obtain this version, we cannot provide further details.

Due to the lower concentration of the titrant, the BrIn is best suited to hydroprocessed POs with low olefin content. For crude POs, required sample charges can drop to ≤10 mg, risking significant errors. Dilution can help, but finding a universal solvent that fully dissolves any PO is challenging. Despite these limitations, several groups report using BrIn for PO characterization, yet many papers describe BrIn but report results in g Br₂/100 g (and label them “bromine number”), raising methodological concerns.

Escola et al. [28–30] state the use of ASTM D2710 (described by the authors as a coulometric method) to monitor the degree of unsaturation in POs after hydrotreatment. Given the terse information (only samples were dissolved at an unknown dilution in an unspecified solvent), suitability cannot be fully assessed. Reported olefin saturation was 80–97 % with Ni catalysts, with BrIn (referred to as BrN) decreasing from 54.1 to 1.4 g Br₂/100 g after 45 min at 310 °C and 20 bar H₂ in a batch reactor [29]. Walendziewski et al. [31] used the withdrawn ASTM D1491 for olefin quantification. Hydrotreating over 0.5 % Pt- or Pd/Al₂O₃ catalysts for PE, PP, PS, and their mixture lowered unsaturation from 88.5 to 0.5 g Br₂/100 g [31]. In tire pyrolysis oil hydrotreatment, unsaturation decreased from 67.5 to 11.1 g Br₂/100 g over sulfided NiMo catalyst at 380 °C and 5 MPa [32].

2.3. Iodine value (IV)

Defined by Von Hübl over 140 years ago [33], the iodine value (IV), often called iodine number or index, quantifies aliphatic C=C via the addition of halogens. Several variants exist (e.g., Hanuš method using iodine monobromide - IBr [34]), but Wijs’ 1898 method using [35] **iodine monochloride (ICl, known as Wijs reagent)** is the most used [35]. In Wijs’ method, **ICl adds cross-aliphatic double bonds (R3)**. This method is standardized as ASTM D5554 and EN 14111 for fats, oils, and fatty acid methyl esters (FAME).



According to both standard methods, the sample is dissolved in a solvent mixture of glacial acetic acid and cyclohexane (1:1 v/v). Then, 25 mL of Wijs solution (0.1 M ICl in acetic acid) is added. As with all titration methods, adjusting the sample size based on the expected IV is recommended to ensure at least 50 % excess of ICl [36]. Due to the lower reactivity of ICl compared to Br₂, the titration mixture is allowed to stand in the dark for 0.5–1 h, allowing the addition reaction to proceed. After that, 20 mL of 10 % KI solution is added, and the unreacted ICl is converted to I₂, whose concentration is determined by titration using 0.1 M Na₂S₂O₃. The double bond amount is then indirectly determined by back titration against a blank. The titration can be performed either visually using a starch indicator until the blue color disappears or more accurately and practically with a potentiometric titrator equipped with a suitable electrode. The results of this method are presented as the grams of iodine required for the titration of 100 g of a sample (g I/100 g).

Applied to fats (often solid at ambient temperature), IV avoids many BrN solubility issues seen for PE-rich POs. The unsaturated structures in fats and oils resemble the long, straight aliphatic chains of PE-derived olefins, making the IV method a promising alternative for PO unsaturation. However, Wijs reagents are more toxic, and the method is slower than BrN, reducing practicality.

The reaction time for the IV determination could be accelerated with a mercury-based catalyst, which was found ineffective for BrN [37]. Wijs [35] used HgCl₂ to generate ICl from I₂ [35], and Hoffman & Green [38] showed Hg(OAc)₂ rapidly promoted ICl addition [38], cutting analysis

to ~10 min, but at the cost of higher toxicity and only marginal IV increase for vegetable oils [38]. Notably, Auersvald et al. [16] demonstrated that $\text{Hg}(\text{OAc})_2$ enables near-quantitative determination of aliphatic double bonds in POs, substantially increasing the reactivity of conjugated dienes and sterically hindered $\text{C}=\text{C}$ [16]. In the JET-A1 spiking test, the modified IV method closely matched true total aliphatic double-bond content and aligned well with the olefin-selective GC \times GC method for real polyolefin POs free of heteroatom compounds (Figs. 1–2) [16].

Interference from phenols, thiophenes, and polyaromatics remains a concern. Removing oxygenates and nitrogenated species over Florisil can partially mitigate overestimation [16], but high polyaromatic and thiophene contents in tire POs still interfere.

Standard IV has been widely used for tire POs [39–42]. Reported IVs span ~20–50 g I/100 g, reflecting process-dependent unsaturation levels and molecular-weight distributions. Short reaction times (e.g., the 5 min Mettler Toledo variant without $\text{Hg}(\text{OAc})_2$) likely understate IV [39,41], consistent with Auersvald et al. [16], and interferences in tire POs often outweigh incomplete olefin reactivity [16].

Like BrN/BrIn, IV decreases with increasing average molecular weight/boiling range: naphtha fractions show the highest IV, while $>360^\circ\text{C}$ bottoms show the lowest [39,40]. For polyolefin-derived POs, IV ~38–84 g I/100 g has been reported [16]. IV can track hydrotreating, with near-complete olefin removal at 330°C and 6–10 MPa over sulfided NiMo [39]. However, because IV relies on back-titration, its sensitivity at very low olefin levels is inferior to BrN, making it less effective for deeply hydrotreated POs.

Greener variants include Hanuš (IBr) method [34], which has been modified to reduce the consumption of titrant and solvent [43], and the Tubino and Aricetti method [44], but their suitability for POs is uncertain. In particular, poor PO solubility in ethanol:water (1:1 v/v) limits the Tubino–Aricetti approach. Overall, solvent choice and analytical conditions require careful optimization for PO analysis [44].

Overall, titration methods represent a relatively fast approach to obtain the quantitative information about the olefinic unsaturation of plastic-derived oils represented by a single value. However, varying interference concentration as well as incomplete reactivity of all olefinic double bonds can significantly affect the accuracy of those standard methods. As the result depends on the average molar weight of olefins, which is directly related to the

boiling point range of the sample, the interpretation and comparability of the results from titrations are not straightforward.

3. Spectroscopic methods

3.1. Fourier transform infrared spectroscopy (FTIR)

FTIR is a rapid, cost-effective technique for identifying olefinic structures in hydrocarbon mixtures, including POs. Although its quantitative use is limited, FTIR provides clear structural fingerprints. For instance, vinyl and vinylidene bands appear between 850 and 1000 cm^{-1} , the $\text{C}=\text{C}$ stretch is near 1650 cm^{-1} , and $=\text{C}-\text{H}$ out-of-plane stretch falls in the 800 – 1000 cm^{-1} region [45–47]. These mostly weak vibrational modes enable selective monitoring of olefins formed during thermal cracking.

Even without absolute quantification, FTIR discriminates samples across processing conditions and fractions. In mild cracking of HDPE and HDPE/PP, Jing et al. [48] observed bands at 1641 cm^{-1} and $909/992\text{ cm}^{-1}$ ($\text{R}-\text{CH}=\text{CH}_2$) concentrated in the light fraction; similar behavior was reported for PP and LDPE/PP mixtures [49]. Thus, monitoring bands of mono-substituted alkenes (≈ 990 and 910 cm^{-1}) and *cis*-disubstituted $\text{C}=\text{C}$ ($\approx 720\text{ cm}^{-1}$) supports relative comparisons of olefin content [47].

Advancements in FTIR technology, particularly mid-IR external-cavity quantum cascade lasers coupled with photoacoustic detectors, have improved sensitivity and selectivity, potentially mitigating some quantitative limitations. However, additional development is needed for routine hydrocarbon analysis [50]. FTIR is widely used to characterize pyrolysis products; in plastic-derived oils, bands near 1575 and 1675 cm^{-1} , and at 875 and 950 cm^{-1} indicate $\text{C}=\text{C}$ stretching, while bands at 887 and 909 cm^{-1} correspond to mono-substituted $\text{C}=\text{C}$ bonds in PP and LDPE cracking products [51].

In co-pyrolysis processes, such as lignite/LDPE/red mud or coal and plastic blends, FTIR helped identify specific functional groups, including aromatic and conjugated olefinic hydrogen (1600 cm^{-1}) and olefinic $\text{C}=\text{C}$ stretching at 1642 cm^{-1} [52,53].

Despite its speed for functional-group screening, FTIR lacks the structural detail and quantification achievable with advanced methods such as GC-MS. Accordingly, it is often paired with GC-MS or NMR to enhance specificity and accuracy in hydrocarbon characterization.

3.2. Raman spectroscopy

Raman spectroscopy is a powerful vibrational technique for detecting $\text{C}=\text{C}$ in olefinic compounds. By probing changes in polarizability, it is highly sensitive to unsaturated groups; the $\text{C}=\text{C}$ stretch appears at ~ 1610 – 1680 cm^{-1} and provides a strong, distinct fingerprint even in complex matrices [54]. Compared with IR, Raman is less affected by water and enables non-destructive, rapid analysis with minimal sample preparation [55]. Its compatibility with fiber-optic probes and adaptability to online monitoring make it well-suited for industrial control of olefin content during polymer or fuel production [55].

Recent works demonstrated that Raman spectroscopy is applicable for characterizing olefins in petroleum-derived and renewable fuels. Gieleciak et al. [54] semi-quantitatively tracked olefins in cracked naphtha and renewable gasoline with detection limits near 1 vol% %, noting that species-dependent Raman cross-sections complicate absolute quantification but can be mitigated with matrix-specific calibration models. Heigl et al. [54] pioneered a quantification approach based on integrating olefin-specific band areas, achieving $\pm 10\%$ accuracy in complex hydrocarbon mixtures [56,56].

Only a few examples address POs or polymer blends directly. Gopanna et al. [57] used Raman spectroscopy to monitor polypropylene blending with cyclic olefin copolymers; by tracking intensity ratios of polymer-specific bands, they confirmed blend uniformity and quantified

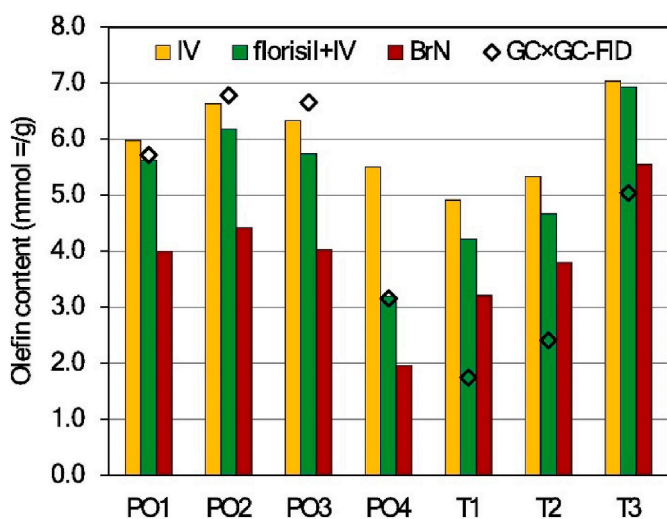


Fig. 2. The result for olefin content for real PPOs. IV Hg-5 min (yellow), Florisil adsorption + IV Hg-5 min (green), BrN (red), and GC \times GC-FID (black rhombus). PO = polyolefin-rich pyrolysis oil, T = tire pyrolysis oil. Reproduced with permission from Ref. [16] Copyright 2025 Elsevier. (For interpretation of the references to color in this figure legend, the reader is referred to the Web version of this article.)

composition without inducing chemical change. Although focused on solid-state blends rather than depolymerization oils, the work illustrates Raman's ability to resolve olefinic features in complex macromolecular matrices. In an industrial setting, Kuptsov et al. [55] demonstrated real-time process control in poly- α -olefin oil production, using Raman to monitor C6–C10 α -olefin oligomerization and track both conversion and molecular-weight distribution [55].

Although direct Raman applications to pyrolysis POs remain scarce, evidence from petroleum and polymer systems indicates that Raman is well suited for qualitative olefin detection and, with matrix-specific calibration, can be adapted for quantitative monitoring in plastic-waste-derived products.

3.3. Nuclear magnetic resonance (NMR)

^1H -NMR is a robust tool for qualitative and quantitative analysis of hydrocarbon mixtures. Olefinic protons resonate at 4.00–6.60 ppm, providing a clear signal for detection and quantification. Integrating the olefinic region relative to the total spectrum yields the **mol% of olefinic hydrogen type**, enabling quantitative estimates of olefin content.

Compared with FTIR, ^1H NMR offers higher selectivity and a direct quantitative approach, albeit at significantly higher capital and operating costs. Results correlate well with established measures such as the bromine number, supporting accuracy and reliability. While short acquisitions suffice for qualitative screening, longer acquisition times or advanced experiments (e.g., 2D NMR) are often required for high-resolution and fully quantitative data. Existing ASTM fuel NMR methods emphasize hydrocarbon class distributions and may not explicitly target olefin monitoring.

^1H NMR has been extensively applied to quantify olefins in fuels, thermal cracking products, and plastic-derived oils, consistently using the 4.00–6.60 ppm window to detect olefinic hydrogens.

Olefin content is critical to gasoline quality, particularly its octane rating. Myers et al. [58] utilized ^1H NMR to derive isoparaaffinic index, olefin vol%, and aromatics vol%, with trends consistent with GC-MS. This demonstrates the robustness of ^1H NMR in fuel analysis, particularly in quantifying olefins without interference from other hydrocarbons [59].

^1H NMR has also been extensively applied to characterize hydrogen types in products from thermal and catalytic cracking of LDPE, HDPE, and PP. In mild cracking of 60/40 HDPE/PP, less than 4 mol% olefinic hydrogens were detected in the supernatant liquid [45], and similar observations were made in LDPE/PP blends, where increasing LDPE content correlated with a higher proportion of olefinic hydrogens [49]. Comparable olefinic hydrogen concentrations were reported for oils from co-pyrolysis of lignite with LDPE and other plastic waste, and from HTL of ocean-derived plastics [47,52,53]. These findings highlight ^1H NMR capability to resolve hydrogen distributions in highly complex mixtures.

It is crucial to recognize that ^1H NMR quantifies hydrogen types rather than olefin molecules. In POs, especially those from PP, olefinic hydrogens are often on branched structures, yielding fewer olefinic H per double bond than linear PE-derived olefins. As with titration methods, lighter (lower-boiling) fractions enriched in low-molecular-weight olefins show higher proportions of olefinic hydrogens than heavier cuts; therefore, a lower mol% of olefinic hydrogens does not necessarily indicate a lower overall olefin content.

Process conditions further shape the hydrogen distribution. Higher reactor fill levels broaden the product boiling range and suppress cyclization, favoring heavier products with more saturated and olefinic hydrogens relative to aromatics. Short residence times limit secondary reactions and preserve longer-chain alkanes and olefins, whereas longer residence times promote additional cracking, cyclization, and eventual aromatization [51]. *Thus, while a dominance of aliphatic hydrogens may suggest limited secondary chemistry, interpretation must account for molecular-weight distribution, branching, and reaction severity; without this*

context, olefin trends inferred from ^1H NMR alone can be misread.

Advanced 2D-NMR, particularly Heteronuclear Single Quantum Coherence (HSQC), correlates ^1H and ^{13}C signals to resolve detailed structures (Fig. 3). For example, HSQC contours at 5.06–5.95 ppm (^1H) and 110–116 ppm (^{13}C) assign $=\text{CH}_2$ groups in styrene and α -methyl styrene [60]. These techniques offer more profound insight into the complex hydrocarbon structures.

Despite its versatility, ^1H NMR has notable limitations. It measures the mol% of olefinic hydrogen rather than the number of olefin molecules and can thus underestimate the olefin content relative to paraffins. Short acquisitions often lack the resolution and accuracy for reliable quantitation, necessitating longer runs or complementary methods. While ^1H NMR usefully captures the whole sample—including species that GC may miss due to non-volatility or thermal instability—its sensitivity is modest: typical detection and quantification limits are $\sim 1\%$, so olefin contents below roughly 10 % in complex matrices are difficult to quantify reliably. Consequently, ^1H NMR is best for relative quantification and comparative studies; absolute quantification in highly complex mixtures generally requires calibration standards, advanced methodologies, or corroboration by other techniques. For context, ASTM D5292 (total hydrogen by NMR) exhibits similar sensitivity constraints, though it is not designed for olefin quantification.

4. Liquid chromatography methods

4.1. Fluorescent indicator adsorption (FIA)

FIA (ASTM D1319) is a **displacement chromatography** method for group-type quantification of samples with boiling points $\leq 315^\circ\text{C}$ (e.g., fossil naphtha, kerosene) [61]. A narrow glass column packed with SiO_2 separates the sample by polarity into saturates, olefins, and aromatics. An indicator dye visualizes zone boundaries under a UV lamp (aromatics are blue, olefins yellow, and saturates colorless); measuring zone lengths in a constant internal diameter of the column yields volume percent (vol %). For a specific example, see Fig. 4.

Key limitations include low throughput (the analysis is time-consuming) and incompatibility with samples having a wide boiling point range (final boiling point $> 315^\circ\text{C}$), where heavier straight-chain or polyaromatic molecules can crystallize on SiO_2 and disrupt the separation. Sensitivity is modest: the ASTM LOD is 1 vol%, which also seems valid for POs [16]. Additionally, the standard specifies that dienes can be identified as either olefins or aromatics, introducing potential bias [61].

Mikulec et al. [22] applied FIA to quantify olefins in gasoline and middle-distillate fractions from catalytic pyrolysis of polyolefins. In the 180–330 $^\circ\text{C}$ cut, PP-derived oils contained 89–95 vol% olefins versus 49–78 vol% for PE. Consistent with this, Soják et al. [23] reported, for thermal pyrolysis, middle-distillate olefins of 93.3 vol% (PP) and 70.4 vol% (PE).

In an aromatics quantification study, Auersvald et al. [15] analyzed a hydrotreated PO sample spiked with typical diene structures (octa-1,7-diene, 2,5-dimethylhexa-2,4-diene, D-limonene, and α -terpinene). None were classified as olefins by FIA; instead, all were assigned to the aromatics zone.

Auersvald et al. [16] compared olefin-determination methods for polyolefins and tire pyrolysis oils and found that FIA accurately quantified all common mono-olefin structures in POs. Within its limitations, FIA produced results comparable to those of GC \times GC-FID, employing olefin adsorption on Ag- SiO_2 [16]. Similarly, Barzallo et al. [62] reported a strong correlation between FIA (acknowledging dienes underestimation) and a newly developed selective-derivatization method, particularly in the gasoline-range fractions of POs.

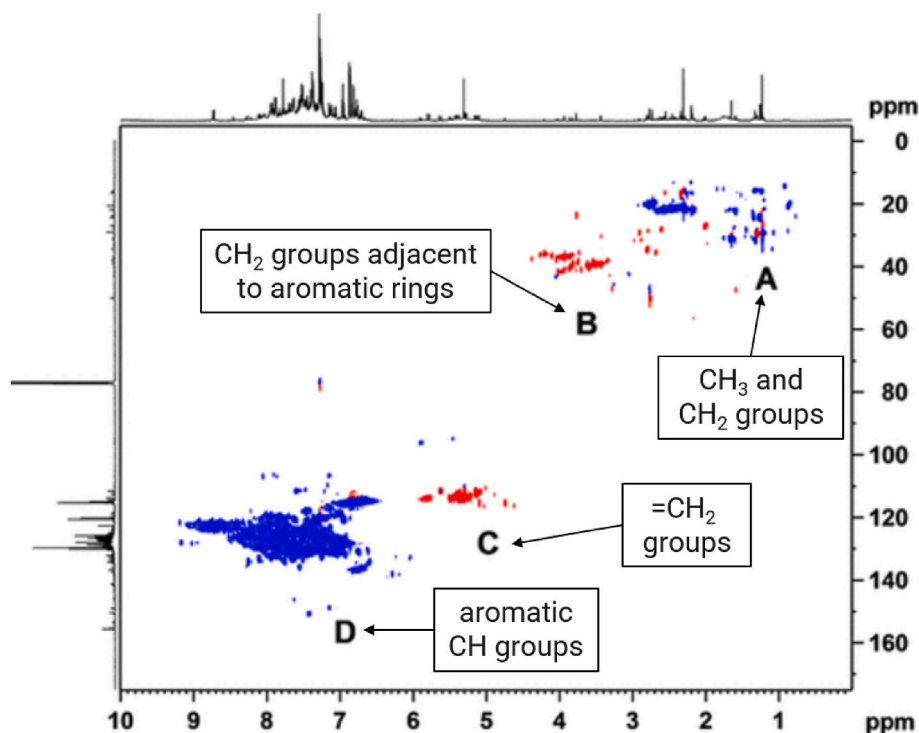


Fig. 3. HSQC spectrum of the hydrocarbon oil produced at 800 °C. Reproduced with permission from Ref. [60] Copyright 2018 American Chemical Society.

4.2. High-pressure liquid chromatography (HPLC)

HPLC is widely used in petroleum and petrochemical analysis to separate hydrocarbons, including olefins. Column choice is critical, and the most common column configuration for separating saturates, olefins, and aromatics is the normal-phase HPLC, with a polar stationary phase (e.g., silica) with a non-polar mobile phase (e.g., hexane).

Detector selection governs identification and quantification. Bulk-property detectors such as refractive index (RI), conductivity, and evaporative light-scattering (ELSD) are common. RI is reliable but limited to isocratic runs due to solvent-composition sensitivity, whereas ELSD offers higher sensitivity and supports gradient elution, making it suitable for middle and heavy distillates [63]. Specific-property detectors expand capability: UV–visible is useful for aromatics and polar species, and fluorescence excels for PAHs, typically in heavier fractions using reversed-phase HPLC [64].

Suatoni et al. [65] developed a preparative normal-phase HPLC for group-type separation of olefins from synfuels, combining high selectivity with scalable throughput. Using a silica column and a perfluoroalkane eluent with RI detection, the method cleanly isolated olefins from saturates and aromatics, yielding highly enriched fractions suitable for downstream analysis or use. Its major drawback was the high cost of the perfluoroalkane [65].

Jinno et al. [66] introduced a more practical variant using reactivated silica and n-hexane at 0 °C, with dual detection (UV for aromatics, RI for total hydrocarbons). Defined elution windows—0–4.7 mL (saturates), 4.7–8.2 mL (olefins), >8.2 mL (aromatics)—improved resolution and reduced cost, making the approach efficient for routine group-type analysis [66].

Building on early HPLC advances, dual detection (RI + UV) improved resolution and specificity, enabling simultaneous quantification of key hydrocarbon classes. These refinements established HPLC as a reliable tool for fuel-quality assessment and refinery applications.

Normal-phase HPLC with RI and UV (240 nm) has been used to quantify olefins and conjugated dienes in gasoline in a single run on a Hypersil silica column (250 × 4.6 mm, 5 µm) with hexane at 1 mL/min.

The method achieved a detection level of 0.02 wt% for total conjugated dienes using 2,4-dimethyl-1,3-pentadiene as the standard (calibration $R^2 = 0.9972$). Olefins are calibrated with 1-octene; however, accuracy degrades below ~10 wt% because RI signals overlap with saturates [67].

An improved normal-phase HPLC protocol quantifies saturates, olefins, conjugated dienes, and aromatics in full-range cracked gasoline (90–230 °C). It uses a WELCH Ultisil HILIC Silica column (250 × 4.6 mm, 5 µm, 100 Å) with hexane at 1 mL/min and calibrants of 1-octene (olefins) and 2,4-dimethyl-1,3-pentadiene (DMP; conjugated dienes). The method delivers improved resolution with minimal coelution; conjugated dienes are monitored selectively at 240 nm (UV) with negligible background from other classes, enabling specific, low-interference quantification. The method is high-throughput, requiring approximately 10 min per sample. Calibration employs structurally representative olefins, *trans*-2-octene and *trans*-2-nonene, selected based on NMR and simulated-distillation profiles to mirror cracked-gasoline compositions. Results correlate closely with FIA, underscoring robustness and suitability for routine analysis [68].

4.3. Supercritical fluid chromatography (SFC)

The ASTM D6550 determines olefin content in motor gasoline and blendstocks via supercritical-fluid chromatography (SFC). Using supercritical CO₂ as the mobile phase, a small aliquot is separated on two serial columns: high-surface-area silica followed by silver-ion-loaded silica (see Section 6.4.1.3) or a strong cation-exchange phase. It quantifies olefins over 1–25 wt% and can report results in vol% or wt% without detailed molecular speciation. Limitations include relying on specialized columns that degrade over time and lacking structural differentiation among olefins. *High sulfur in tire-derived oils can rapidly deactivate the Ag⁺ column*. Reported reproducibility from one application note [69] ranges from 0.5 to 5.3 wt% olefins, following the relationship: reproducibility = $0.47 \times (\text{olefin wt}\%)^{0.75}$.

Kaplitiz et al. [70] used SFC–UV (220 nm) to analyze and differentiate olefin-containing POs from PE and PP. Optimizing 2-ethylpyridine



Fig. 4. FIA analysis of chosen samples – CKF = kerosene fraction of crude pyrolysis oil from films (left); KF3 – kerosene fraction from pyrolysis oil from PE films after hydrotreatment at 360 °C and 6 MPa (right). Reproduced with permission from Ref. [15] Copyright 2024 Elsevier.

columns and coupling them in series yielded distinct chromatographic fingerprints. Although UV at 220 nm does not directly quantify alkanes/olefins, it highlights aromatics and N/O/S species. Across nine POs, PP-derived oils showed higher olefin content (~60 %) and formed distinct PCA clusters, enabling estimation of PE:PP ratios in mixtures. Compared with GC–FID, whose signals are dominated by alkanes, SFC–UV provided clearer differentiation. Limitations remain: UV cannot

directly quantify alkanes/olefins, so coupling to MS could improve molecular identification. Future work could include PS-derived oils and developing a fingerprint database to support machine-learning POs classification [70].

Liquid chromatographic (LC) methods are valuable alternatives to GC for quantifying olefins in POs and cracked gasoline. FIA (ASTM D1319) separates saturates, olefins, and aromatics by polarity with UV–visible indicators, but it is time-consuming, limited to streams with final boiling points ≤ 315 °C, and excludes dienes from the olefin fraction, often classifying them as aromatics. In contrast, normal-phase HPLC on silica with hexane enables faster (~10 min per sample), more flexible group-type analysis. Using RI and/or 240 nm UV detection with representative standards supports reliable quantification of olefins and conjugated dienes, and results correlate well with FIA, making HPLC suitable for high-throughput work. SFC (ASTM D6550) employs supercritical CO₂ and silver-ion-loaded silica to quantify olefins across 1–25 wt% without molecular speciation. Limitations of HPLC and SFC include non-uniform detector responses and the shortened lifetime of Ag⁺ columns, which are sensitive to sulfur commonly present in POs. Nevertheless, SFC has proven useful for compositional fingerprinting of POs, enabling differentiation between PP- and PE-derived products.

5. Gas chromatography (GC) methods

Although GC methods probe only the volatile fraction, they provide superior molecular resolution, enabling detailed identification and quantification of individual olefins compared with other techniques.

5.1. Conventional (1D) GC

One-dimensional GC (1D-GC), a single-column setup, is **the workhorse for PO characterization**. Because its peak capacity is limited relative to GC \times GC, it is best suited to **lighter streams** (like gas and naphtha) typical of catalytic pyrolysis. Numerous standardized methods are available for these matrices.

5.1.1. Gaseous products

Commercial Refinery Gas Analyzers (multicolumn GC) are widely used to characterize gaseous olefins. Although some species (e.g., ethylene) can be seen on the TCD channel [71], the most detailed results come from FID with alumina PLOT columns (typically 30–50 m \times 0.32–0.53 mm \times 5–10 μ m). Standardized methods such as ASTM D2163 and UOP 539 apply, and because the number of isomers is limited, method adjustments are rarely required.

Retention order varies slightly by manufacturer but generally follows the degree of unsaturation for a given carbon number: alkane < alkene < alkyne (acetylene) < diene. Alumina columns are commonly deactivated with KCl, proprietary treatments (e.g., HP-PLOT M or Q), or Na₂SO₄; the latter increases alkyne retention. Columns are sometimes paired in series with a non-polar phase. As summarized in Table S1, elution orders can differ across application notes. Because alumina columns are limited to ~200 °C, they are typically used for C1–C6, with heavier material handled by backflush as a C6 or C7+ cut. Depending on configuration, run times are fast, about 10 to <30 min.

Although gaseous-analyte identification is straightforward, accurate quantification is more demanding given the limited species set and established elution orders. Routine calibration of response factors and retention times with certified gas mixtures is essential. For the best mass balance and superior accuracy/precision, online analysis of continuous-process gases is recommended [72–74].

The most accurate workflow spikes the effluent with a known internal-standard mass flow, typically nitrogen, which is often used as an inert in pyrolysis [51,75–82]. The RGA's TCD channel quantifies N₂, enabling the determination of methane; methane can then serve as a

secondary internal standard for other species on additional GC channels. This steam-cracking procedure is detailed by Van Geem et al. [83]; see the summary in Fig. 5.

The automatic valve box on an RGA, enabling automated sampling and complex gas analyses, can be costly. A simpler, lower-cost alternative is to collect outlet gas in a Tedlar bag for offline GC analysis [75, 77–80,84–90]. If the GC has a valve-loop sampler, injecting from the bag after **pressure equilibration** introduces minimal error. In contrast, syringe withdrawals are slower and require operator skill for reproducible results. Ballice et al. [91,92] described GC analysis using a specially designed sample-introduction system as another option [91, 92].

Several groups have utilized alumina columns to study plastic pyrolysis, employing all major deactivation schemes: KCl [87–91], proprietary treatments [85,92], and Na₂SO₄ [78,79,86].

In contrast to alumina columns, which provide higher retention and allow room-temperature separation of light hydrocarbons, an alternative is a long (50–100 m) non-polar capillary column. Adequate resolution of the lightest hydrocarbons typically requires cryogenic oven cooling. A long non-polar column is often more versatile for online pyrolysis analysis because it can also be used directly for heavier products. On non-polar phases, separation follows increasing boiling point; see the C5-hydrocarbon elution order on a 100 % PDMS column in Table S1.

For example, Ballice et al. [93,94] utilized a 50 m OV-1 column with an initial oven temperature of –80 °C, achieving excellent separation of ethylene/ethane and propylene/propane. *In our experience, a 50 m PONA column starting at 30 °C provides adequate C2–C3 resolution; the only significant coelution among lighter compounds is trans-2-butene with 2-methylprop-1-ene.* Elordi et al. [95] reported detailed C4 separations on a PONA column (length not specified) with a 35 °C start.

Olefins yield in pyrolysis depends strongly on the reactor type, temperature, hold time, feedstock, and catalytic promotion. Raising the temperature to 700 °C increases gas formation, with olefins as the dominant hydrocarbons [95,96]. In closed batch systems, olefin formation is suppressed in favor of secondary reactions such as hydrogen transfer (increasing the yield of paraffins) and increased cyclization/aromatization [97]. Light-olefin production is strongly enhanced by catalytic pyrolysis with zeolites, most commonly ZSM-5 [98–102]. Eschenbacher et al. [103] reported up to 85 wt% C2–C4 olefins (ethylene 16.5 wt%, propylene 46 wt%, C4 olefins 22.5 wt%) from mixed polyolefin waste and LDPE at 550 °C with pyrolysis vapor upgrading over boron-modified mesoporous HZSM-5.

5.1.2. Liquid products

For light (naphtha) fractions and catalytic pyrolysis products, routine gasoline group-type analysis on a PONA column is appropriate.

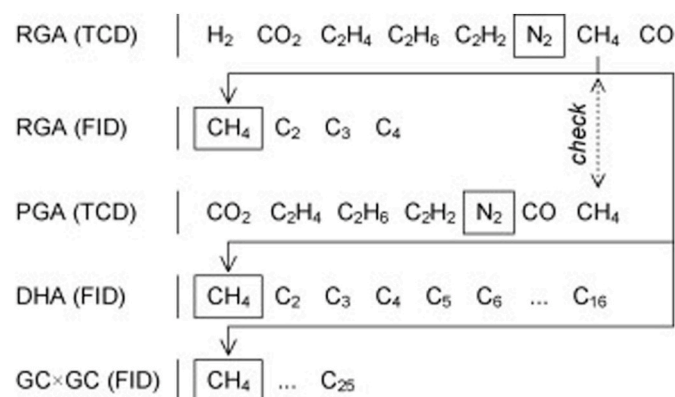


Fig. 5. Use of reference components for quantitative online effluent analysis in a refinery gas analyzer (RGA) setup employing programmed-gas analyzers (PGA) and detailed hydrocarbon analysis (DHA) channels. Reproduced with permission from Ref. [83] Copyright 2010 Elsevier.

The method is standardized as ASTM D6729 (100 m, 100 % PDMS) and D6733 (50 m, 100 % PDMS). Long non-polar columns provide near-complete, boiling-point-based separation of analytes up to C10. For fossil gasoline, the standards list the elution order of most components; analytes are then grouped by structure into *n*-paraffins, iso-paraffins, olefins, naphthenes, and aromatics, hence the P(I)ONA designation.

The C5 elution order is summarized in Table S1. For details, see ASTM D6729, ASTM D6733, or an open-access Restek note [104]. Annex A1.1 of ASTM D6729 lists the elution order of >400 hydrocarbons typical of fossil gasoline. Although olefins are included up to C10, PO streams rich in olefins require substantial database expansion because > C7 olefins are uncommon in standard fossil gasoline. The limitations of 1D-GC-FID detailed hydrocarbon analysis (DHA) versus olefin selective GC-VUV were confirmed by Dunkle et al. [105], who showed DHA can overestimate or misassign olefins even in fossil naphtha.

In our experience, 1D-GC-FID with a PONA column per ASTM D6733 has significant shortcomings for accurate olefin quantitation in POs, even within the naphtha fraction (<150 °C). A more reliable approach is the parallel use of GC-MS and GC-FID [88] utilizing the same column and GC conditions for compound identification and quantification. While we found no study explicitly describing the simultaneous use of FID and MS detectors on 1D-GC, several plastic recycling reports use both detectors with identical column setups across separate runs [72,73,80,106–109].

The most common approach for PO composition is 1D-GC-MS, which reports relative olefin percentages based on Total Ion Current (TIC) area ratios [23,46,48,75,85,86,90,110–118]. Although these TIC abundances are often presented as weight percent (wt%) [18,76,119, 120], it is important to note that **TIC area% ≠ wt%**. Even in hydrocarbon-rich POs, where MS response factors vary less than in biomass-derived bio-oils [121], the differences between TIC area% and FID wt% can still be significant [111]. Notable quantitative efforts include primarily the deuterium-labeled internal standards method published by a South Korean group [106,122–124]. A recent Serras-Malillos et al. [125] study highlighted a significant limitation of the commonly used GC-MS quantification approach that assumes area% = wt%. To address this, the authors developed a methodology based on commercially available calibration mixtures, enabling GC-MS determination of compounds in POs while accounting for the entire oil composition.

Although FID responses are more uniform than MS across hydrocarbons, they still depend on the compounds' C/H ratio. Accordingly, the standard PONA methods recommend correcting compound responses using **relative response factors (RRFs) calculated through the effective carbon number (ECN) approach** [125,126]. The RRF can be determined using Equations (1)–(3).

$$RRF(CH_4) = \frac{MW_i}{Nc^*} \cdot \frac{1}{MW_{CH_4}} \quad (1)$$

$$Aci = Ai \cdot RRFi \quad (2)$$

$$\%Wi = \frac{Aci}{\sum_{i=1}^{i=n} Aci} \cdot 100 \quad (3)$$

Where.

RRF (CH₄) = response factor relative to methane

MW_i = molar weight of component *i*

Nc = effective carbon number for heteroatom-containing compounds*

*The number of carbons contributing to the response must be calculated according to the corrections mentioned in the following articles [125,126].

% Wi = percent weight of the component *i* in the mixture

Aci = corrected area

A_i = acquired area for an individual component [119,120].

Most GC-FID studies report simple FID area% as wt%. This approximation can be reasonable for largely aliphatic, low-heteroatom POs from polyolefins completely eluting out of the column. However, when aromatics are more abundant, as in catalytic pyrolysis oils [28,76,122,127,128], feeds containing PS, PET, and/or PVC [18,85,87,106], tire thermal depolymerization oils [39,129,130], or real-waste oils containing heteroatoms, response factors are needed for accurate quantification. Notably, only one 1D-GC-FID study to date has applied the ECN-based RRFs for quantification [80].

It has been shown that 1D-GC-MS can distinguish *n*-paraffin, linear olefins, and branched olefins during mixed-plastic pyrolysis monitoring [90]. However, as molecular weight increases, single-column peak co-elution becomes a significant limitation, restricting quantification to mainly *n*-alkanes and α -olefins, typically present at high concentrations in polyolefin-derived oils [94]. For PE pyrolysis oils, Berrueto et al. [119] identified three dominant families at each carbon number: *n*-paraffin, α -olefin, and α,ω -diene, with α -olefins being the most abundant (see Fig. 6).

Distinguishing olefins from naphthenes in EI mass spectra is challenging because their fragmentation patterns are similar, which casts doubt on some literature reports. During plastic pyrolysis, cracking and cyclization occur. Only a few 1D-GC studies reported naphthenes in POs [76,97,106,109,110,112,116] and even unsaturated naphthenes [106,117]. Fraczak et al. [18] differentiated *i*-olefins from naphthenes in PP oils by MS fragmentation only up to C10; above C10, both were combined due to insufficient distinction. The limited resolution of 1D-GC leads to peak co-elution, especially for low-abundance species, and likely underpins questionable compositions and unusual identifications in some reports [114,131]. *Based on our experience with POs and bio-oils from biomass pyrolysis, even with near-ideal GC \times GC separations, library matches require critical review; wherever possible, match retention indices against NIST or literature values to ensure reliable assignments.*

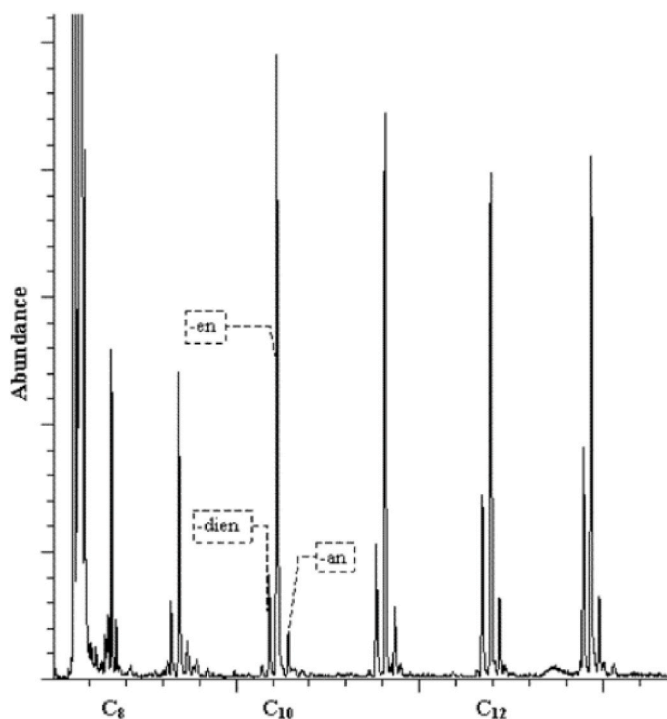


Fig. 6. GC-MS chromatogram of wax + oils derived from pyrolysis of HDPE showing the characteristic triplets of alkenes, alkanes, and alkadienes. Reactor temperature 650 °C; residence time of 0.8 s. Reprinted with permission from Ref. [119]. Copyright 2002 American Chemical Society.

Soják et al. [23] provide the most comprehensive PO compositional analysis to date, even with simple 1D-GC. Using a 150 m Petrocol DH column with a thicker film (1 μ m) and a constant 1 °C/min ramp, they achieved near-perfect peak separation that enabled exact identification and naming of 52 octene isomers from PE pyrolysis oil. Beyond the usual *n*-paraffins, α -olefins, and α,ω -dienes for each carbon number, they also resolved and quantified E-alk-2-ene and Z-alk-2-ene in PE oil. The study offers an excellent analysis of MS fragmentation patterns for the major PP-derived olefin structures (see Fig. 7), and together with chromatograms, retention indices, and spectra, serves as an invaluable resource for compound identification in polyolefin pyrolysis oils.

In the 1D-GC studies above, non-polar columns (typically 95–100 % PDMS, ~30 m) are used. To increase resolution in these complex matrices, several groups employed longer non-polar columns: 50–60 m [90,93,94,132,133], 100 m [28,109,112,116,127,134] and even 150 m [23]. Polar phases are less common, with examples including a 30 m DB-35 ms [46], a 60 m VF-1701 ms [80], and a unique 30 m VF-200 ms with trifluoropropyl stationary phase [135].

Beyond MS and FID detection, VUV detection, though still relatively rare, can selectively determine olefins in POs using 1D-GC [136]. For more details about GC-VUV methods, see Section 6.1.

5.2. Comprehensive two-dimensional gas chromatography (GC \times GC)

GC \times GC offers substantially higher resolution than 1D-GC, approaching almost complete separation and significantly reducing co-elution. Its growing use in process labs reflects its usefulness for characterizing complex hydrocarbon matrices, such as POs. Coupled with TOFMS and FID, GC \times GC enables confident identification and robust quantification, particularly in the saturated region. *n*-Alkanes, iso-alkanes, *n*-/iso-mono-olefins, diolefins, and naphthenes can be individually resolved and quantified, though typically via labor-intensive peak-by-peak curation. However, as shown by a recent study utilizing selective adsorption of olefin over Ag-SiO₂ (see section 6.4.) [10] even when using a reverse phase GC \times GC column configuration allowing almost perfect separation in the olefin elution region, complex samples like POs are characterized by significant coelution between olefins and saturated compounds.

Dr. Van Geem's group tackles plastic-waste recycling end to end: waste sorting and pretreatment [137,138], thermal [21,89,139] and catalytic [102,103,140] pyrolysis using py-GC \times GC; pilot-scale studies [21,89,139,141,142], pyrolysis oil upgrading [5,143], and final conversion to monomers via steam cracking [141,144,145]. This multifaceted strategy is complemented by advanced quantitative analysis of POs using GC \times GC. One of the first studies to apply GC \times GC for detailed PO characterization, including olefins quantification, was published by Toraman et al. [9].

Most of Van Geem's group studies employed a liquid CO₂ GC \times GC modulator and multiple detectors [9,17,142]. FID quantification uses an internal standard (3-chlorothiophene) and ECN corrections (see Equations (1)–(3)). Compounds are identified by qMS or TOF-MS, quantified individually, and then grouped by carbon number and class (as *n*-paraffins, *i*-paraffins, α -olefins, *i*-olefins, diolefins, mononaphthenes, dinaphthenes, monoaromatics, etc.). A reversed-phase column configuration (StabilWax \times Rxi-5ms) proved optimal for the middle-distillate POs, effectively separating diolefins from iso-olefins and mononaphthenes, and separating oxygenates from the hydrocarbon matrix [17] (see Fig. 8) [17]. However, even with slower oven ramps and helium flow, fully resolving the lightest hydrocarbon groups (e.g., *n*-paraffins vs. α -olefins) remains challenging.

Because separating light components is difficult, and the wax column is limited to 260 °C, subsequent studies adopted a normal phase (NP) column configuration (e.g., PONA or Mxt-1 paired with BPX-50 or ZB-35HT) [21,89,102,103,139–142]. Although NP typically compresses the *n*-paraffins and monoaromatics spacing, it remains preferred for

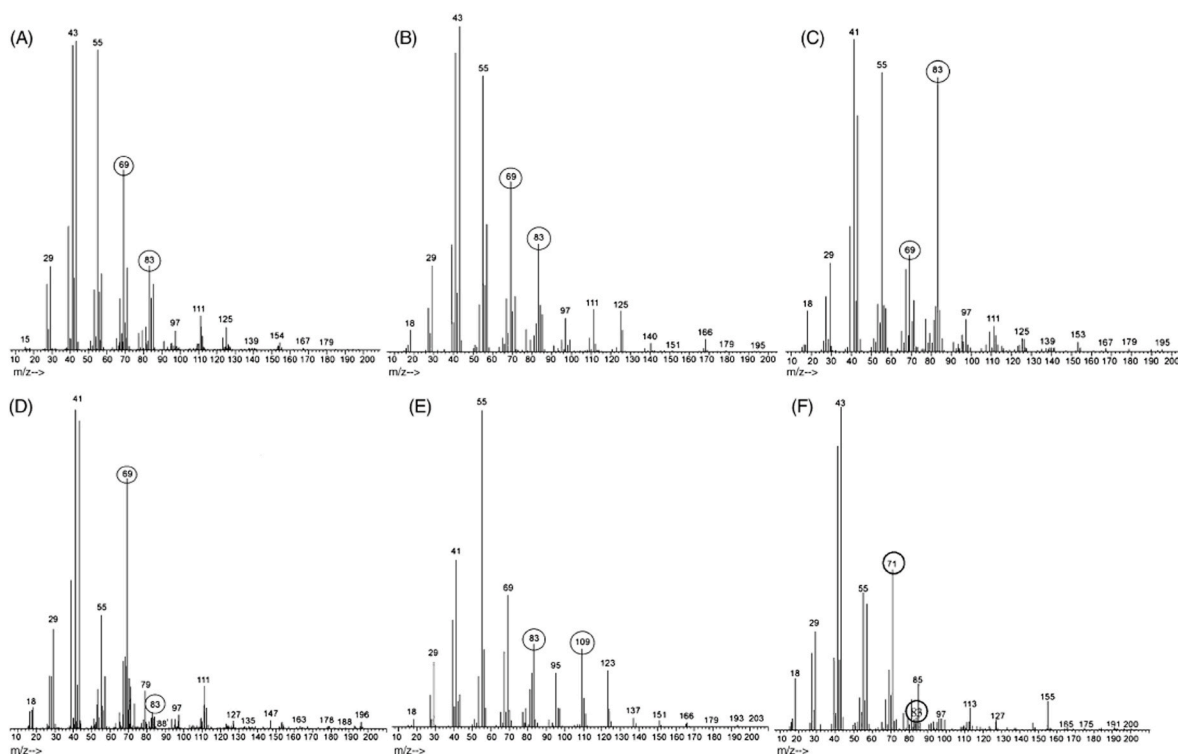


Fig. 7. Mass fragmentation of propylene oligomers. $3n$ alk-1-enes (A), $3n + 1$ alk-1-enes (B), $3n$ alk-2-enes (C), $3n + 2$ alk-2-enes (D), $3n + 1$ alka- α,ω -dienes (E), and $3n + 2$ alkanes (F) with signed specific MS ions. Reproduced with permission from Ref. [23] Copyright 2007 Elsevier.

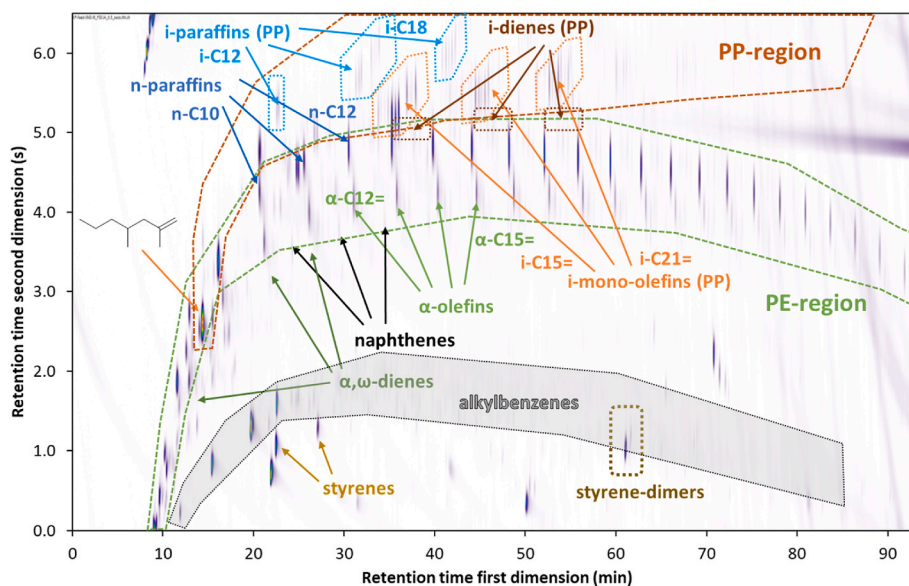


Fig. 8. GC \times GC-FID chromatogram (reverse phase configuration VF17 \times DB-1) of real waste polyolefin-rich pyrolysis oil. Adapted based on refs. [10,17].

broad boiling-range samples, especially mildly cracked polyolefins.

A key challenge is distinguishing diolefins and unsaturated naphthenes with the same molecular masses and near-identical EI fragmentation patterns, complicating GC \times GC-MS identification [17]. Even so, with Mxt-1 + ZB-35HT and a PTV injector, NP minimized sample discrimination and enabled detection up to C75 hydrocarbons [142].

A representative GC \times GC chromatogram for mixed-polyolefin pyrolysis oil is shown in Fig. 9 [143]. PE products display a triplet for each carbon number, α,ω -diene, α -olefin, and n -alkane, while PP products show $3n$ patterns. Typical group-type compositions for PE, PP, and mixed polyolefin waste (MPO) appear in Fig. 10 [143], and a PS

pyrolysis-oil chromatogram is available in the literature [89].

Dr. Wang's group, in collaboration with **Dr. Vozka's group**, develops advanced hydrothermal processing (HTP) and low-pressure hydrothermal processing (LP-HTP) routes for converting polyolefin waste into clean fuels and value-added products, using GC \times GC coupled with FID and TOFMS to analyze the resulting complex hydrocarbon. A central challenge in olefin quantitation is the limited selectivity of GC \times GC-FID, which cannot fully distinguish olefins from cycloparaffins; these are therefore often reported jointly as "olefins and cycloparaffins." To improve resolution, selected studies [146] employ GC \times GC-HRTOFMS to differentiate n -alkanes and α -olefins in HTP waxes, revealing

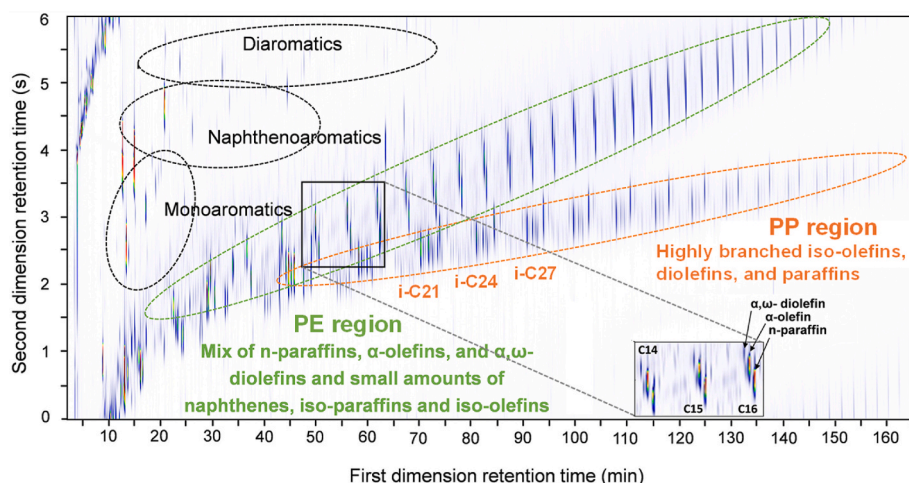


Fig. 9. GC \times GC-FID chromatogram (normal phase configuration Mxt-1 \times ZB-35HT) of mixed polyolefin rigids pyrolysis oil. Reproduced with permission from Ref. [143]. Copyright 2022 Elsevier.

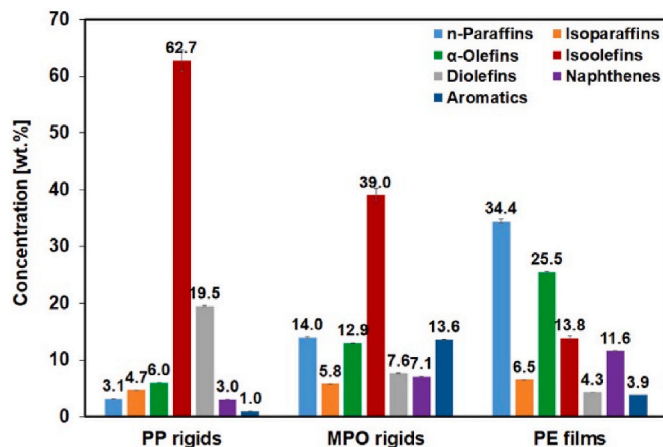


Fig. 10. Hydrocarbon composition of the pyrolysis oils measured using GC \times GC-FID (including standard deviation). Reproduced with permission from Ref. [143]. Copyright 2022 Elsevier.

compositions typically consisting of ~ 80 wt% *n*-paraffins and ~ 20 wt% α -olefins in the C20–C40 range.

Their work quantifies olefins across hydrothermal and pyrolysis-derived oils: HTP of PE and PP yields fuel-range hydrocarbons and waxes [147]; LP-HTP of mixed polyolefin wastes (including disposable face masks) produces clean gasoline and diesel fractions [148]; and mechanistic studies highlight olefins as key intermediates in thermal decomposition pathways [146]. Quantitative analysis used GC \times GC-FID, reporting concentrations from FID peak area %. Compound identities were assigned by TOFMS using mass spectral features such as allylic cleavage, McLafferty rearrangements, and characteristic fragment losses, as well as hydrocarbon classification based on retention time and fragmentation patterns, which allowed differentiation between olefins, paraffins, and cycloparaffins. Olefins were the major constituents of the oils and waxes, with their distribution strongly influenced by temperature, pressure, and feedstock. For example, higher temperatures during HTP tend to promote the conversion of olefins into more saturated and aromatic products.

In 2024, Perez et al. [149] investigated primary PP decomposition with py-GC \times GC-FID/TOFMS, coupling a micropyrolyzer to GC \times GC for real-time analysis of pyrolysis vapors. Using an Rtx-DHA \times Rxi-17 Sil setup, they resolved C3–C35 hydrocarbons and identified >600 products, including paraffins, olefins, naphthenes, diolefins, cycloolefins,

bicyclic compounds, and aromatics. Olefin quantitation employed the ECN approach to ensure accurate response factor calibration.

Wu et al. [150] used GC \times GC-FID to analyze six groups in pyrolysis oils: linear hydrocarbons, branched alkanes, branched alkenes, branched alkadienes, aromatics, and polyaromatics, further subdividing linear hydrocarbons into alkanes, alkenes, and alkadienes via complementary 1D-GC. Validated combined DHA for C4–C10 and nitric oxide ionization spectroscopy (NOISE) evaluation for C10+. For C5–C10, GC \times GC-FID and DHA yielded consistent profiles: alkane maxima at C6–C7 and elevated alkenes at C6–C8. Minor DHA differences (slightly higher alkenes and an “unknown” fraction) likely reflect coelution and limited resolution. GC \times GC provided superior separation and structural detail.

For C10–C35, GC \times GC-FID and NOISE also agreed on alkene distributions, peaking at C15–C17 and tapering at higher carbon numbers. NOISE reports only total alkenes (no structural speciation) and slightly overestimates around C16–C18 with minor deviations beyond C25, consistent with resolution/detector limits. Overall, NOISE is effective for rapid bulk olefin quantification, while GC \times GC remains the preferred tool for detailed compositional analysis [150].

Ureel et al. [151] quantified olefins primarily by GC \times GC-FID, enabling detailed PIONA profiling with accurate compound-level totals. Ultrahigh-resolution Fourier Transform Ion Cyclotron Resonance Mass Spectrometry (FT-ICR MS) complemented this approach by extending molecular characterization to high-molecular-weight species (up to \sim C82) and heteroatom-rich compounds. However, high-resolution MS cannot reliably distinguish hydrocarbons of identical nominal mass (e. g., olefins vs. naphthenes), risking misclassification, and variable ionization efficiencies limit results to semi-quantitative trends.

GC methods are widely used to analyze POs, offering effective characterization of volatile fractions and detailed insights into olefin content and distribution. Conventional 1D-GC is frequently employed for its simplicity and suitability for lighter fractions, such as gaseous and naphtha-range products. Refinery Gas Analyzers equipped with alumina columns and FIDs enable detailed quantification of gaseous olefins, though accurate results depend strongly on proper calibration and standardized procedures. ASTM methods D6729 and D6733 are commonly applied for liquid products based on non-polar PONA columns. However, they face limitations due to co-elution and difficulty distinguishing closely related hydrocarbon classes. GC \times GC, particularly when coupled with TOFMS and FID, offers a step change in resolution and accuracy, effectively overcoming the co-elution limitations inherent in 1D-GC. As a result, GC \times GC has become essential in identifying and quantifying olefins and related hydrocarbons in complex samples

from pyrolysis and hydrothermal processes. Nonetheless, careful use of response factors, internal standards, and advanced detection strategies remains crucial for achieving accurate and reliable compositional data.

6. Selective methods for olefin analysis

6.1. GC and GC \times GC with vacuum ultraviolet (VUV) spectroscopy

VUV detection offers a powerful alternative to FID and MS for complex samples such as POs. Commercialized in 2014 [152,153] by VUV Analytics, VUV detectors operate from 120 to 240 nm [154], with newer models (e.g., VGA-101) extending to 430 nm [155]. Hydrocarbons show distinct deep-UV spectra, enabling classification by functional group and subtle structural differences.

The determination using VUV primarily relies on **relatively fast GC analyses** using a non-polar column without specific efforts to eliminate analyte co-elution. VUV chromatogram is subsequently deconvoluted, with the **time interval deconvolution (TID)** method representing the most frequently used approach for PIONA group-type analysis. The fully automated TID algorithm, commonly applied today, was described in detail by Walsh et al. [156]. It divides the chromatogram into time-slice intervals, each assigned specific retention indices. VUV spectra from the library corresponding to each retention index window are then used to generate a deconvoluted chromatogram, accounting for RRFs of various compound classes or species.

Compared to traditional GC detectors, **VUV excels at distinguishing olefins from naphthenes**, which are not easily distinguishable by EI-MS and prone to coelution even in GC \times GC. Various olefin types (mono-olefins, conjugated dienes, and isolated dienes) exhibit unique VUV spectra, allowing for precise identification (Fig. 11). Curated spectral libraries further enhance group-type analysis and even distinguish constitutional isomers of small hydrocarbons [157]. With operator assistance, C₈H₁₈ isomers were correctly identified at concentrations of \sim 0.2 wt% [158]. Recent work also demonstrates that GC-VUV can accurately quantify specific diolefin isomers in plastic pyrolysis oils, including linear α,ω -diolefins and branched diolefins [159].

VUV detection has gained significant attention in recent years, enabling several standardized group-type methods for hydrocarbon fuels (ASTM D8071, D8267, D8369) and, in July 2023, ASTM D8519 for

plastic pyrolysis oils. The comprehensive overviews are available in recent reviews [156,157,160]. Because VUV is mass-sensitive and follows the Beer–Lambert law, it supports calibration-free, pseudo-absolute quantification [161]. RRFs are often applied in practice, though variability within hydrocarbon classes can affect accuracy [158,162,163]. The main limitation remains the modest spectral library (\sim 2000 unique compounds) [157,160]. Sensitivity and dynamic range are also inferior to FID, for example, 1-octene LOD \approx 0.1 wt% and a dynamic range of only \sim 2–3 orders of magnitude [137]. A detailed summary of VUV constraints is provided by Lelevic et al. [137,160].

Expanding the VUV spectral library is critical for better quantifying complex POs rich in isomers and heterocompounds. While TD-DFT-based spectral prediction (Mao et al.) shows promise [164], recent machine-learning approaches outperform it [165]. A practical complement to library growth is experimentally determining RRFs via parallel FID/VUV measurements [162]. Coupling VUV with GC \times GC further improves accuracy by reducing co-elution. Although VUV can scan at 100 Hz [152,157], GC \times GC applications typically use \sim 33–50 Hz to lower noise and improve sensitivity [162,163,166].

Despite its advantages, VUV remains underutilized in plastic-recycling research, with only a few PO studies to date [25,137,167]. The VGA-101 detector is well-suited for these applications due to its high maximum operating temperature (up to 430 °C), which minimizes the risk of analyte condensation during analysis [155]. For example, Lazzari et al. [167] utilized GC-VUV to validate the differentiation of naphthenes from olefins identified by GC \times GC-PI-TOFMS (see following section). Ureel et al. [159] demonstrated GC-VUV's efficacy for analyzing hydrotreated pyrolysis POs, accurately quantifying and identifying diolefins and olefins across C7–C27. Detailed GC-VUV analysis has demonstrated an explicit dependency of hydrogenation rates on chain length and branching structure, underscoring the need for accurate quantification of structural isomers [159].

Dunkle et al. [137] compared olefin content obtained by GC-VUV and bromine number (BrN) titration for mixed-waste pyrolysis oils, reporting a linear correlation. However, several critical limitations raise concerns about the reliability of those conclusions. *The study did not report sample origins or heteroatom content, affecting spectral interpretation and titration accuracy. The conversion of BrN values to wt% olefins was based on assumed average molecular weights without disclosure of the methodology, an approximation noted in ASTM D1159 Annex A2 but*

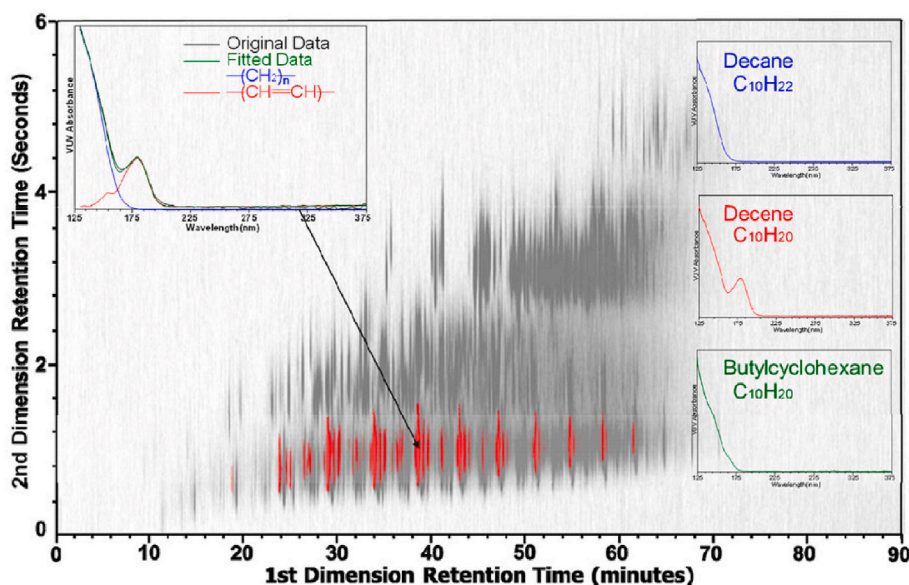


Fig. 11. The Distribution of olefins (red) in a Coker diesel sample's saturated polarity area in GC \times GC \times VUV. (Insets) VUV seed spectra for olefins, paraffins, and one-ring naphthenes were used in the deconvolution. Reprinted from Ref. [157] under the terms of the CC BY-NC-ND 4.0. No changes were made to the original image. (For interpretation of the references to color in this figure legend, the reader is referred to the Web version of this article.)

unlikely to hold for heterogeneous POs. A more rigorous comparison would calculate mmol of double bonds directly from detailed GC–VUV data. Furthermore, the BrN titration was conducted at 25 °C instead of the ASTM-specified 0–5 °C, likely increasing side reactions with polyaromatics and compromising selectivity, as the authors acknowledged.

Despite these issues, GC–VUV remains a promising tool for olefin quantification in POs thanks to its speed and group-type resolution. Broader adoption, however, will require key improvements: expansion of reference spectral libraries, systematic evaluation of RRF variability across olefin structures, and investigation of VUV absorption by highly branched iso-alkanes and propylene oligomers. The influence of heteroatom-containing species (N, O, S) in real waste POs also remains poorly understood. Finally, coupling VUV detection with GC × GC could greatly enhance separation, particularly in the C5–C20 range, reducing reliance on spectral deconvolution and improving analytical robustness.

VUV spectroscopy is an emerging and promising tool for hydrocarbon analysis, particularly for complex mixtures like POs. Its

ability to distinguish olefins and other hydrocarbon classes surpasses traditional GC-MS and FID methods, but challenges remain in library expansion, quantification accuracy, and sample complexity. Several studies also lack critical evaluation, often omitting details about which compounds were added to the spectral libraries or how their RRFs compared to existing data. Addressing these limitations will be key to unlocking the full potential of VUV for olefin analysis in POs.

6.2. Soft ionization mass spectrometry

As discussed in section 5, excessive fragmentation in MS detectors operating at the standard EI energy of 70 eV prevents the selective identification of all olefins present in POs. **Soft ionization techniques** mitigate this issue by **reducing fragmentation** while preserving the ability to **distinguish naphthenes from olefins**. Among the available soft ionization methods, including cold-EI, chemical ionization (CI),

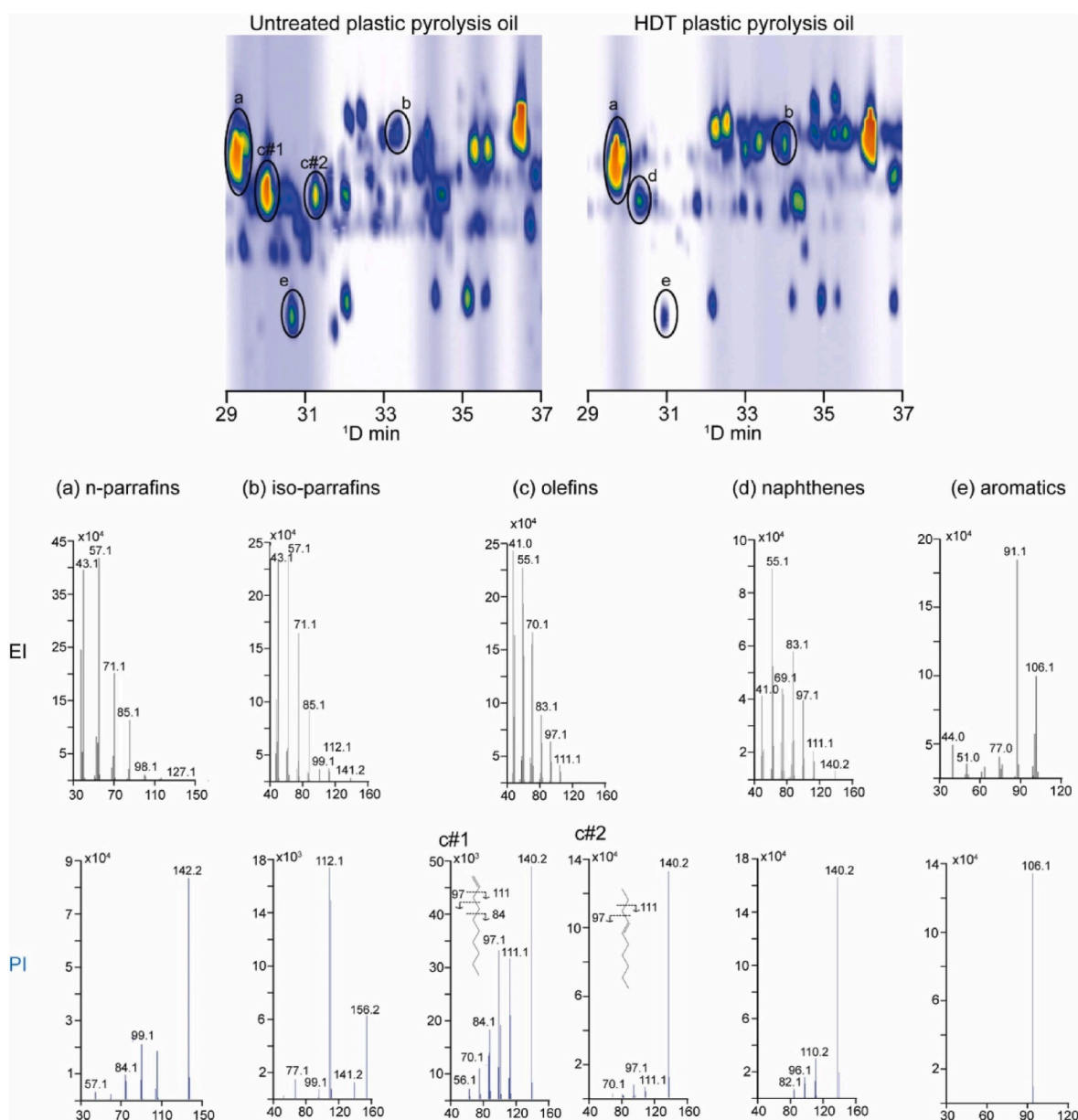


Fig. 12. Partially zoomed total ion chromatogram (TIC) of an untreated pyrolysis plastic oil and an HDT pyrolysis oil analyzed by GC × GC-EI/PI-TOF MS. Mass spectra comparison of EI vs PI for selected (a) C10 n-paraffins, (b) C11-isoparaffins, (c) and (d) C10-olefin congeners, (e) C10-naphthenes, and (f) aromatics. For olefins, probable molecule structures and the breaking site are indicated. Reprinted from Ref. [167]. Copyright 2023 Elsevier.

field ionization (FI), and photoionization (PI) [167–172], PI is currently **the most widely used** for resolving isomeric structures in complex hydrocarbon mixtures.

PI-MS spectra are characterized by strong molecular ion signals along with informative fragmentation patterns [168,170]. When coupled with GC \times GC, which provides near-complete analyte separation, PI ionization provides a powerful approach for the selective identification of olefins, including the determination of double-bond positions and branching [167,168]. For example, Zou et al. [169] analyzed dodecene mixtures and described the predominant cleavage types (α , β , and γ) observed during the PI of various linear and branched dodecene isomers.

Lazzari et al. [167] used GC \times GC-PI-TOFMS to characterize crude and hydrotreated POs from mixed plastic waste. PI-MS resolved species that overlap in EI-MS: naphthenes, olefins, dienes, and unsaturated naphthenes. Olefins show diagnostic alkyl-chain-cleavage fragments, whereas cyclohexane rings yield characteristic ions at m/z 82, 96, and 110. Representative spectra are shown in Fig. 12.

Beccaria et al. [168] used high-resolution GC \times GC-PI-TOFMS to characterize mixed PO, enabling detailed identification of olefin isomers, including the number of double bonds and branching degree/-position. Increasing branching significantly reduces compound retention times, with highly branched C24 iso-olefins and a C25 iso-diene eluting earlier than C19 and C20 *n*-alkanes, respectively [1].

While soft ionization offers promise, one alternative is lowering the EI energy. Burdová et al. [173] demonstrated that lowering EI energy to 12–15 eV did not resolve naphthenes from olefins in pyrolysis POs. Amirav et al. [174] likewise found that reducing EI energy has a limited impact on enhancing molecular-ion intensity. Generally, when the molecular ion is absent at 70 eV EI, lowering the energy generally does not recover it. By contrast, cold EI may offer reliable olefin identification,

similar to PI. To our knowledge, as of September 2025, no peer-reviewed study applied cold-EI MS to POs, based on a targeted literature search by the authors. We therefore highlight cold-EI as a promising yet untested option for olefin identification in POs.

6.3. Derivatization of olefin double bonds

Derivatization of olefins improves their selective identification and quantification in GC analyses, especially in complex hydrocarbon matrices such as petroleum oils. Direct analysis of olefins in these mixtures is difficult because their non-polar nature leads to co-elution with structurally similar naphthenes and close elution with paraffins in GC \times GC separations. In addition, olefins often show limited detectability and specificity with conventional detectors such as FID, and may interfere with or be obscured by other compounds in titration-based methods.

Derivatization—chemical modification to enhance detectability or alter chromatographic behavior—helps address these challenges. Introducing functional groups increases polarity, improving separation from naphthenes and paraffins. Derivatized olefins also yield more informative and distinctive MS fragmentation patterns, producing selective ions that support compound identification and structural elucidation. In some cases, derivatization enables alternative selective detectors beyond MS, depending on the functional group introduced.

A wide range of derivatization strategies targeting C=C has been developed, as reviewed comprehensively in Ref. [175]. The choice of method depends on the analytical objective—whether the priority is improved chromatographic separation, enhanced MS detectability, or selective detection with other detectors. The most common approaches are summarized in Fig. 13 and include the methods summarized in the following sections.

Silylation reaction was first described by Sommer et al. [176] in

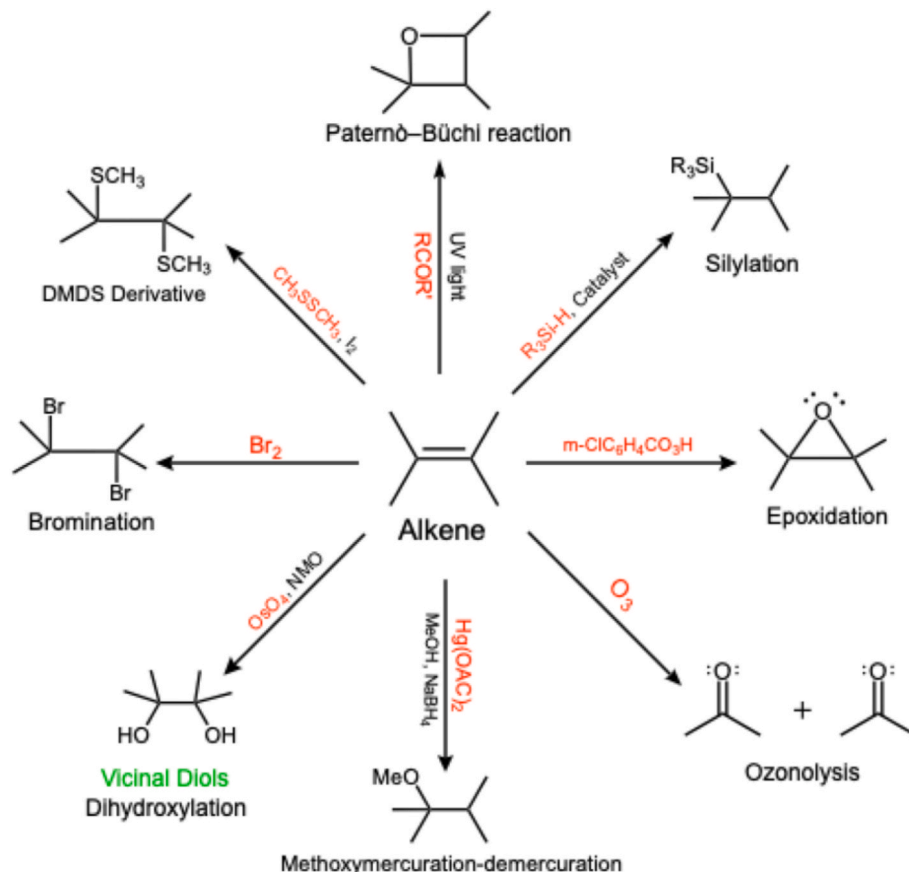


Fig. 13. A reaction scheme of alkene derivatization.

1947, where trichlorosilane was reacted with 1-octene using peroxide to initiate a free-radical process. However, the reaction was noted for its relatively low selectivity [176,177]. Common silylating agents include trichlorosilane (HSiCl_3), trimethylsilane (HSiMe_3), and triethylsilane (HSiEt_3), depending on the desired selectivity and application. The silylated derivatives are analyzed using MS, where the resulting mass spectra reveal ions that provide information about the original compound's structure, including the position of functional groups and double bonds [175]. It is essential to note that compared to hydroxyl group silylation (O-TMS), typically producing a characteristic fragment ion at m/z 73 (trimethylsilyl cation), the silylation of olefins yields distinct fragmentation patterns dependent on the specific silylating agent and the olefin's structure. Potential interference from alcohols or other functional groups must be considered, as overlapping signals in mass spectra can complicate analysis [178].

Epoxidation is based on the reaction of an olefin with a peroxycarboxylic acid, such as *m*-chloroperoxybenzoic acid, to form an epoxide. The resulting epoxide can then be analyzed using MS, which often exhibits characteristic fragmentation due to cleavage near the oxirane ring. This method is particularly valuable for determining the position and geometry of double bonds in aliphatic compounds. Though this method is mainly effective for alkenes with one double bond, it can be extended to more complex compounds, providing insights into their structure and enhancing the reliability of subsequent analyses, such as GC-MS [179,180]. The epoxides can also be analyzed using chemical ionization gas chromatography/mass spectrometry (CI-GC-MS), where the mass spectra typically reveal abundant $[\text{M} + \text{H}]^+$ ions along with pronounced diagnostic fragment ions [175,181]. For example, in the case of unbranched aliphatic epoxides such as epoxydecane, ring cleavage produces prominent fragment ions at m/z 157 ($[\text{M} + \text{H}]^+$ with subsequent loss of a neutral fragment), m/z 139 (resulting from further cleavage of the alkyl chain), and m/z 87 (representing a hydrocarbon fragment derived from ring cleavage). These specific ions provide information about the position and configuration of the epoxide group [179].

In **ozonolysis**, a carbon-carbon double bond in olefins is cleaved by ozone (O_3) to yield oxygenated species such as aldehydes, ketones, or carboxylic acids. This transformation enhances their detectability by GC-MS and is particularly valuable for locating double bonds in isomeric olefins. In the study by Xie et al. [182], online ozonolysis was coupled with single-photon ionization time-of-flight mass spectrometry (SPI-TOFMS) to enable real-time, solvent-free identification of double bond positions. The SPI method, utilizing a krypton discharge lamp (10.6 eV), enabled soft ionization and minimized fragmentation, thereby preserving molecular ion peaks and diagnostic fragments.

For example, *n*-heptanal, produced by the ozonolysis of 1-octene, yielded a molecular ion at m/z 114, along with key fragment ions at m/z 96 (loss of H_2O), m/z 86 (loss of C_2H_4), and m/z 72 (loss of C_3H_6). Similarly, ozonolysis of *cis*-2-octene resulted in *n*-hexanal (m/z 100) and acetaldehyde (m/z 44), while *cis*-3-octene generated *n*-pentanal (m/z 86) and propanal (m/z 58). These fragments are essential for identifying the original double bond location. In addition to molecular ions, the fragment m/z 44 is specific for the McLafferty rearrangement of aldehydes.

Older GC-based methods, such as those [183] developed by Beroza and Bierl [183], also effectively characterized ozonolysis products at the microgram level using FID. They confirmed similar aldehyde generation (e.g., heptanal from 1-octene) and reported that compounds like acetaldehyde were more challenging to detect due to their volatility and lower FID response. Despite that, ozonolysis products such as acetone and propionaldehyde were readily identifiable from sub-microgram quantities.

Methoxymercuration-demercuration represents another derivatization for identifying double bond positions in unsaturated compounds. In this two-step reaction, the unsaturated sample first undergoes methoxymercuration by treatment with mercury (II) acetate in

methanol, followed by reduction with sodium borohydride (demercuration), ultimately resulting in methoxy-substituted derivatives. These derivatives can then be analyzed using MS. This approach is particularly effective for monounsaturated compounds, as each double bond incorporates a single methoxy group, facilitating clear identification of double bond positions based on characteristic fragmentation patterns. For example, methoxy-substituted fatty acid methyl esters commonly exhibit intense diagnostic fragment ions at m/z 74 (McLafferty ion: $\text{CH}_3\text{OCH}_2^+$) and characteristic fragments indicative of cleavage adjacent to methoxy substitution sites, such as m/z 87, 101, or 115, depending on the alkyl substituents present. However, analyzing polyunsaturated compounds is more challenging, as each double bond undergoes independent derivatization, resulting in complex mixtures of mono-, di-, or tri-methoxy derivatives and corresponding complex spectra. Hydrogenation of polyunsaturated compounds before derivatization simplifies this complexity by reducing the number of reactive double bonds, yielding partially or fully saturated derivatives that are easier to interpret by mass spectrometry [175,183]. A notable disadvantage of this method is the toxicity and environmental hazard posed by mercury (II) acetate, necessitating stringent safety precautions during handling, usage, and disposal [184].

Dihydroxylation (OsO_4): Catalytic osmium tetroxide (OsO_4) oxidation in the presence of co-oxidants such as *N*-methylmorpholine *N*-oxide (NMO) is a stereospecific reaction for converting alkene double bonds into *cis*-1,2-diols (vicinal *cis*-diols). This transformation is beneficial in structural elucidation studies and the synthesis of bioactive compounds. However, due to their polarity and propensity for dehydration under EI conditions, *cis*-diols exhibit poor GC performance and complex EI-MS fragmentation patterns [185,186]. To overcome these challenges, common derivatization approaches involve the formation of *O*-isopropylidene (acetonide) derivatives, significantly enhancing chromatographic behavior and simplifying spectral interpretation. The resulting acetonide derivatives display characteristic fragmentation patterns primarily involving β -cleavage adjacent to the dioxolane ring, leading to diagnostic ions stabilized by adjacent ether functionalities. Typically observed fragments include m/z 185 and m/z 213, indicative of characteristic ring-cleavage products. Additional diagnostic ions are generated through sequential neutral losses of functional groups, such as acetic acid (60 Da) or methanol (32 Da), leading to ions at, for example, m/z 267 and m/z 235, which facilitates the localization of the original double bond position. Despite its utility, the dihydroxylation method has limitations, including the inherent toxicity, volatility, and high cost of OsO_4 , which necessitate using catalytic amounts with suitable co-oxidants. The necessary derivatization step adds complexity to sample preparation, though it significantly improves chromatographic and mass spectral analysis [187].

Dimethyl Disulfide (DMDS) derivatization was introduced by Carlson et al. [188]. The method involves the iodine-catalyzed addition of DMDS across the double bonds, forming stable bis(methylthio) derivatives. Typically, the reaction proceeds at room temperature over 24 h, though elevated temperatures (e.g., 60 °C for 4–6 h) can significantly accelerate the reaction. The resulting DMDS adducts can be directly analyzed by GC-MS [188,189]. EI MS fragmentation occurs preferentially at the carbon-carbon bonds adjacent to the sulfur atoms, generating two diagnostic fragments whose masses indicate the original position of the double bond. For instance, the DMDS derivative of (*Z*)-9-heptacosene yields diagnostic fragment ions at m/z 173 and m/z 299, the sum of these fragments equaling the molecular ion ($\text{M}^+ = 472$). Similarly, the DMDS derivative of terminal olefins, such as 1-tetradecene, generates characteristic fragments at m/z 61 and m/z 229, clearly indicating the terminal position of the double bond [190]. This derivatization approach is highly effective for analyzing various saturated compounds, including monoenes, dienes, and trienes, and is particularly useful for complex biological and synthetic mixtures. Nonetheless, the method has several limitations, notably reduced reactivity with methyl-branched double bonds due to steric hindrance, as

bulky substituents impede the addition of the second $-\text{SCH}_3$ group. Furthermore, polyunsaturated compounds can form poly- or cyclic DMDS adducts, complicating spectral interpretation. Despite these limitations, DMDS derivatization remains a precise, reliable, and versatile tool for elucidating double bond positions in unsaturated hydrocarbons across numerous analytical applications [186,190].

Bromination is a selective chemical method employed for profiling olefins through the selective addition of bromine (Br_2) to carbon-carbon double bonds, forming vicinal dibromoalkanes. This selectivity is critical, as olefins react rapidly and efficiently, whereas saturated hydrocarbons (alkanes) remain largely unreactive, and aromatic compounds exhibit significantly reduced bromination under controlled reaction conditions. Typically, bromination is performed at low temperatures (0 – 5°C) in non-nucleophilic solvents, such as pentane, to minimize side reactions and unwanted radical substitution. Following the reaction, the residual bromine is quenched using an aqueous sodium thiosulfate solution to prepare the sample for analysis. While highly selective, the reaction is not entirely exclusive to olefins; although typical alkene conversions exceed 99.5 %, minor bromination of aromatic compounds (~ 6.7 %) can occur due to radical-mediated pathways [191].

GC \times GC-TOFMS can analyze the brominated products. Extracted ion chromatograms (EICs), focusing on characteristic ions of brominated derivatives, highlight these species clearly, while total ion chromatograms (TICs) provide broader sample profiling. A discovery-based comparative approach known as tile-based F-ratio analysis is employed to enhance the detection of olefin-derived dibromoalkanes in complex matrices (e.g., gasoline). This analysis compares chromatographic tiles from original and brominated samples, specifically identifying regions where olefins disappear and corresponding dibromoalkanes emerge. Due to their distinct retention behavior and characteristic fragmentation patterns (e.g., intense bromine isotopic clusters at m/z 107/109 and characteristic alkyl fragments), compounds such as 1-pentene and 1-hexene are easily identified as their dibrominated derivatives. This approach further enhances analyte detection by revealing brominated derivatives in chromatographically less crowded regions [191,192].

Paternò-Büchi (PB) reaction is a photochemical $[2 + 2]$ cycloaddition of an aliphatic carbon-carbon double bond with an electronically excited carbonyl group, typically from a ketone such as acetone or benzophenone, under UV irradiation, producing a four-membered oxetane ring. The introduction of this oxetane moiety notably increases the polarity of originally nonpolar olefins, significantly enhancing their detectability via soft ionization methods, such as atmospheric pressure chemical ionization (APCI), which is frequently paired with ultrahigh-resolution mass spectrometry (UHRMS). PB-derived oxetane derivatives exhibit distinct and predictable fragmentation patterns. Typical fragmentation routes involve oxetane-ring cleavage and sequential alkyl chain losses, yielding diagnostic fragment ions commonly observed at m/z 119, 145, 173, and 205, depending on the alkyl substituents and structural complexity of the derivatized olefins. These characteristic fragmentation pathways provide accurate structural insights, enabling clear differentiation of olefins from structurally similar hydrocarbons, including naphthenes and aromatic compounds, within complex mixtures such as fluid catalytic cracking (FCC) slurry oils. The combination of PB derivatization with APCI-UHRMS is particularly advantageous, as it significantly improves chromatographic behavior, ionization efficiency, and consequently the detectability and characterization of high molecular weight olefins, extending analytical coverage to hydrocarbons as large as C_{50} [193].

These derivatization strategies broaden the range of detectable olefins and offer detailed molecular insights into their structural features and composition. The summary of fragmentation patterns can be found in Table S2. Foundational studies provide valuable resources for understanding fragmentation patterns, underlying reaction mechanisms, and the effective integration of derivatization approaches with advanced analytical techniques [175,194]. Seban et al. [195] present a

comprehensive review of derivatization methods tailored explicitly for GC and GC-MS, illustrating their practical applications and highlighting their analytical advantages in complex sample analysis.

6.4. Selective separation of olefins via complexation with silver ions

Silver ions (Ag^+) form π -complexes with olefin $\text{C}=\text{C}$ via vacant d-orbitals, i.e., a Lewis acid-base interaction where Ag^+ acts as the acid and the π -electrons are the base [180]. Numerous separation strategies have been developed, with chromatographic techniques being among the most established. In these methods, π -complexation with Ag^+ significantly enhances separation efficiency and selectivity. Sid-phase extraction (Ag^+ -SPE) has also been demonstrated beyond column-based argentation as a practical route to isolate olefins from paraffins in heavy, highly overlapping hydrocarbon matrices, as detailed below [196].

In addition to chromatographic systems, ionic liquids (IL), primarily aqueous solutions of Ag^+ + salts, have also been explored as an alternative separation medium. In such systems, olefins can be selectively extracted into the IL phase, or the IL can be combined with membrane separation processes, an emerging and promising approach that has gained growing attention in recent years. These and other methods are discussed in more detail in the following sections.

6.4.1. Chromatographic techniques

Separation based on the π -complex formation over solid materials, such as adsorbents or membranes, is widely applied across various fields of chemistry. In chromatographic applications, silica gel is the most commonly used support for immobilizing Ag^+ , typically introduced as AgNO_3 . In this setup, Ag^+ ions are exchanged onto the silica surface by coordinating with the oxygen atoms of the silanol group. The nitrate anion lies flat against the silica, forming three hydrogen bonds with adjacent silanol groups, stabilizing the surface's ion pair [197]. This interaction between Ag^+ and the silica matrix is reversible and is illustrated schematically in Fig. 14.

In argentation chromatography, non-polar solvents like n -hexane [198,199] and n -heptane [163,200] elute saturates from analyzed samples. Olefins and aromatic compounds are subsequently eluted using polar solvents. Examples include ethyl acetate [198], a mixture of dichloromethane and methanol [163], or individual solvents like dichloromethane or methanol [199].

The stability of the complex depends on the electron density around the double bond and the overall molecular structure. For example, substituents on the double bond reduce the electron density, decreasing

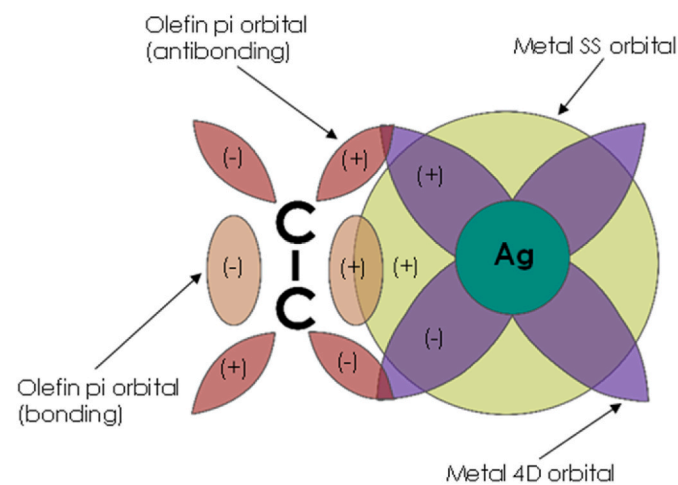


Fig. 14. Illustration of π -complexation between an $\text{Ag}(\text{I})$ ion and an olefin. Reproduced with permission from Ref. [201]. Copyright 1993 American Chemical Society. The figure has been colored to improve clarity.

the complex stability and, consequently, the retention volume during chromatography [202]. However, the instability of metal ions under certain conditions limits separation based on the interaction between double bonds and silver ions. Heat, light, hydrogen, hydrogen sulfide, and acetylenic compounds can reduce Ag^+ ions to metallic silver, compromising olefin selectivity [203].

It was shown that in addition to silver ions, chloride salts of Cu(I) and Au(I) impregnated on silica gel also exhibit strong retention of olefins during liquid chromatographic separation [204]. Additionally, under identical chromatographic conditions, the retention behaviors of unsaturated compounds with Cu(I), Ag(I), and Au(I) are remarkably similar. In practice, AgNO_3 -impregnated silica HPLC/SFC columns can suffer from limited lifetimes (often < 2–3 months under routine use) due to gradual loss or deactivation of Ag^+ , motivating simpler, more robust implementations of Ag^+ complexation for sample prep and class separation [196].

Chromatographic separation of olefins via π -complexation with silver-modified stationary phases can be achieved through various techniques, such as preparative column chromatography, thin-layer chromatography, SPE, HPLC, SFC, and GC. The SFC method utilizes an Ag-modified column and is standardized for olefin determination in gasoline fuels as ASTM D6550. More details about this method are mentioned in section 4.3.

6.4.1.1. Liquid chromatography (LC). Preparative argentation LC on silica gel at 80 °C selectively separates high-molecular-weight saturates from unsaturates (aromatics and resins) in crude oils and outperforms pure silica or alumina for the saturates [200]. Long-chain olefin separations are often benchmarked on paraffin/olefin model mixtures; AgNO_3 -impregnated zeolite, with uniformly dispersed AgNO_3 , cleanly resolves olefins up to C10 [205]. For more complex matrices, AgNO_3 -alumina has been used to isolate olefins up to C28 in shale oils after prior aromatic removal on alumina columns [206], while AgNO_3 -silica has enabled trace-olefin detection in crude oils and environmental monitoring of synthetic-based drilling muds. Sequential normal-phase silica (for aliphatic separation) followed by AgNO_3 -silica further fractionates alkanes and olefins [207].

Silver-ion preparative chromatography has also been applied to isolate olefin-rich fractions from FCC gasoline for subsequent NMR and GC-MS analysis [198]. A similar technique was used for separating C20–C25 olefins from high-boiling Fischer-Tropsch products [199]. Similarly, preparative LC on Ag-modified silica was applied to pre-separate saturates and unsaturates in FCC and coker gas oils prior to GC \times GC-FID, enabling differentiation of naphthenes from olefins; results agreed well with GC \times GC-VUV analyses [163].

Ag^+ -SPE is a robust alternative for heavy matrices. In contrast to AgNO_3 -impregnated analytical columns, Ni et al. [196] established a solid-phase extraction (SPE) workflow using Ag^+ -exchange resin cartridges to separate paraffins and olefins in the saturate fractions of coal tar and petroleum coker oil prior to instrumental analysis. The procedure preconditions Ag^+ -SPE cartridges, elutes paraffins with n-pentane and subsequently olefins with dichloromethane, and achieves near-quantitative recoveries for both classes while cleanly reducing GC overlap at higher carbon numbers; this enables confident downstream GC-MS, GC-FI-TOFMS (molecular-ion profiling), and ^1H NMR (olefin type distributions) assignments. Their results show, for example, significant concentration of iso- α -olefins in coker oil but negligible in coal tar and demonstrate the method's value for isomer-level interpretation once paraffin/olefin classes are physically separated.

Practically, Ag^+ -SPE offers (i) short setup time and low cost, (ii) tunable stringency via solvent choice and cartridge series configuration to minimize carryover, and (iii) applicability to heavy and highly complex cuts where 1D GC co-elution hampers quantification. These characteristics make Ag^+ -SPE a transferable sample-prep step for POs prior to GC \times GC-FID/TOFMS or NMR, complementing the Ag^+ -

chromatography literature summarized above [196].

Argentation can also target gaseous olefins: silver-loaded mesoporous silica selectively adsorbs ethylene over ethane, with performance governed by surface area and Ag^+ dispersion [208]. For liquid long-chain olefins, argentation TLC is widely used, often automated or semi-automated, with on-line detection (typically FID) for quantification. Stability of Ag(I) on chromatographic rods improves when using silver thiolate instead of silver nitrate, offering superior light stability and shelf life; this has been demonstrated for separating fatty acid methyl esters and polyaromatics [209].

Silver-impregnated silica HPLC cleanly separates and quantifies olefins and diolefins in gasoline and thermally cracked naphtha [210]. It also serves as a preparative step to isolate olefins from oligomerized products before GC \times GC, enabling clear differentiation of naphthenes from olefins [211]. The method applies across gasoline, kerosene, and diesel fractions and shows good agreement with bromination-based assays.

Supercritical fluid chromatography (SFC) coupled with GC \times GC has been used to fractionate and analyze olefins in complex middle distillates; silver-loaded silica columns in SFC provide baseline separation of saturated vs. unsaturated hydrocarbons, enabling detailed quantification of olefins and other groups [212]. Complementarily, Qian and Di Sanzo [213] demonstrated multi-dimensional SFC with FID and FI-TOFMS: a silver-modified silica column first separates hydrocarbons in SFC; FID quantifies using near-uniform response factors, while FI-TOFMS supplies intact molecular ions for precise composition and structure, effectively resolving isomeric overlaps between olefins and naphthenes.

Muller et al. [214] applied GC-FIMS for automated, detailed characterization of petroleum- and plastic-derived fuels, combining mid-polar GC separation, soft ionization to limit fragmentation, and DBE-based identification. However, because DBE groups olefins and naphthenes (DBE = 1–3) together, this approach can misclassify and overestimate olefins. Broadly, these methods are limited by challenges in distinguishing closely related hydrocarbon classes, reliance on accurate response factors, and potential biases from ionization-efficiency variations.

6.4.1.2. Gas chromatography. Argentation can also be implemented in GC for olefin/paraffin separation using silver-based ionic liquids as the stationary phase [215]. This approach is limited to light olefins because the phase's thermal stability caps at ~125–150 °C, reflecting ionic liquids' relatively low melting points. As in LC, ionic-liquid phases doped with copper can enhance olefin selectivity; notably, Cu^{2+} interacts more strongly with olefins than Cu^+ [216].

A silver(I)-containing GC stationary phase has also been deployed as the second dimension in GC \times GC, enabling separation of complex mixtures (alkynes, dienes, terpenes, esters, aldehydes, ketones) with superior resolution versus conventional nonpolar/polar sets and resolving previously coeluting species [217]. The approach has likewise been applied to unsaturated fatty acid mixtures.

6.4.1.3. Absorption techniques. Beyond adsorption on solids, liquid-liquid extraction with Ag(I)-containing ionic liquids (ILs) has been widely explored [218,219]. Aqueous AgNO_3 -based IL phases selectively extract cyclohexene and other alkenes via $\text{Ag}^+-\pi$ complexation, producing three layers with olefins enriched in the Ag^+ IL at the bottom [218].

Silver-olefin complexation in aqueous AgNO_3 has been probed by ESI high-resolution MS, enabling rapid, straightforward determination of olefin molecular weights in petroleum middle distillates [220]. The approach was recently applied to C10–C50 olefins from thermal cracking of residual paraffinic oil, using ESI-Orbitrap-MS with d_8 -naphthalene as an internal standard for semiquantitative analysis; results correlated well with ^1H NMR [221].

In addition to extraction, silver-based ionic liquids combined with membranes are extensively studied for olefin separation [218,219,222, 223]. Two membrane types dominate. Immobilized liquid membranes (ILMs) dissolve metal ions in a solvent to act as olefin carriers, delivering high selectivity and rapid transport but suffering instability from solvent evaporation [203,224]. Polymer membranes with fixed carrier sites use ligand-exchange mechanisms to facilitate olefin permeation; while more stable, their gas flux is limited by slow diffusion and can be degraded by impurities (e.g., water) in the absorbent phase [225].

6.4.2. Application to products from thermal depolymerization of plastic waste

To our knowledge, only one study has applied olefin complexation for selective PO analysis. Auersvald et al. [10] used an Ag-SiO₂ SPE cartridge to adsorb aliphatic C=C species in microscale. With DCM eluent, monoaromatics bearing aliphatic double bonds (e.g., styrenes) were retained, while alkylbenzenes passed through. Olefins and styrenes contents were then indirectly quantified by GC×GC-FID from signal loss in the corresponding regions of the 2D chromatogram. The approach is reliable for samples with >5 wt% olefins; C5–C6 olefins are somewhat overestimated due to volatility, and aliphatic oxygenates (alcohols, ketones) can cause a slight positive bias.

Despite these caveats, the method is practical for quantitative use and especially for rapid qualitative tracking. It identifies olefins without MS, cutting cost and avoiding time-consuming EI (70 eV) spectral interpretation, and, in practice, delivers higher accuracy for olefins than EI-MS. In a recent study, results correlated well with iodine value titration using Hg(OAc)₂ catalysis [16]; see Section 2.3 for titration details.

In conclusion, silver-ion chromatography is a robust, versatile platform for separating and analyzing olefins across gaseous and liquid streams, including pyrolysis oils and petroleum fractions. By exploiting Ag⁺– π -complexation, it delivers efficient, highly selective separations that support industrial, research, and environmental applications. Paired with Ag⁺-SPE sample prep, the workflow improves quantitative confidence and sharpens isomer assignments in complex matrices.

7. Conclusions

Accurate olefins quantification in plastic-derived products remains a critical analytical challenge. Although traditional titration methods (such as bromine number and iodine value) offer rapid, low-cost assessments, they suffer from limited selectivity, sensitivity to sample composition, and significant interferences. Spectroscopic techniques, including FTIR and ¹H NMR, provide valuable qualitative information but are often constrained by quantification challenges in complex matrices. Chromatographic methods, particularly GC and GC × GC, have significantly improved olefin characterization, with the latest advances in selective detection (VUV, soft ionization MS) and targeted derivatization strategies offering new pathways for detailed molecular-level analysis.

Nevertheless, persistent gaps remain in standardization, the handling of isomeric olefins, and the quantification of olefins in high-boiling and heteroatom-rich fractions. Future progress will require the development of validated multi-technique workflows, greater emphasis on quantitative cross-validation (e.g., combining selective adsorption, soft ionization, and GC × GC methods), and the adaptation of emerging technologies such as real-time spectroscopy and machine learning-assisted chromatographic deconvolution. We recommend validated multi-technique workflows that combine (i) selective adsorption (Ag-SiO₂) or derivatization for selective isolation of olefins, (ii) GC × GC with VUV (fast PIONA, olefin/naphthene discrimination) and PI-MS (detailed speciation and double bond position), and (iii) orthogonal quantitation (e.g., modified IV with Hg(OAc)₂, where appropriate) for cross-checks. Priorities for standardization include: (1) unified units and

reporting (wt%, mmol C=C per 100 g), (2) agreed ECN/RRF sets for olefin subclasses, (3) spectral-library expansion for VUV/PI and publication of open-access reference datasets, (4) documented handling of heteroatom-rich matrices, and (5) benchmark materials spanning volatility/boiling range. Bridging these gaps is essential to enable more accurate, reliable characterization of recycled plastic-derived oils and to support their broader valorization as fuels and chemical feedstocks for steam cracking.

CRedit authorship contribution statement

Miloš Auersvald: Writing – review & editing, Writing – original draft, Data curation, Conceptualization. **Genesis Barzallo:** Writing – review & editing, Writing – original draft. **Hung Gieng:** Writing – review & editing, Writing – original draft. **Jyotika Patel:** Writing – review & editing, Writing – original draft. **Ananya Sharma:** Writing – review & editing, Writing – original draft. **Kevin M. Van Geem:** Writing – review & editing, Funding acquisition. **Petr Straka:** Writing – review & editing, Writing – original draft. **Petr Vozka:** Writing – review & editing, Writing – original draft, Supervision, Resources, Project administration, Funding acquisition, Conceptualization.

Declaration of generative AI and AI-assisted technologies in the writing process

While preparing this work, the authors used Grammarly and ChatGPT to improve the readability and language of the manuscript. After using these tools, the authors reviewed and edited the content as needed and take full responsibility for the content of the published article.

Funding

This work has been partially supported by the National Science Foundation with Award HRD-2112554. We also thank the CSULA Office of Research, Scholarship and Creative Activities for the Minigrant Award. Miloš Auersvald and Petr Straka acknowledge financial support from the state budget of the Technology Agency of the Czech Republic under the programs SIGMA DC2 (project TQ15000068) and TREND 1 (project FW01010158), respectively. The work was supported by the Ministry of Education, Youth and Sports of the Czech Republic from the institutional support of the research organization (CZ60461373). This project has received funding from the European Union's Horizon 2020 Research and Innovation programme under grant agreement No. 101058412 (HEU-ELECTRO).

Declaration of competing interest

The authors declare that they have no known competing financial interests or personal relationships that could have appeared to influence the work reported in this paper.

Appendix A. Supplementary data

Supplementary data to this article can be found online at <https://doi.org/10.1016/j.trac.2025.118463>.

Data availability

No data was used for the research described in the article.

References

- [1] J.E. Rorrer, G.T. Beckham, Y. Román-Leshkov, Conversion of polyolefin waste to liquid alkanes with Ru-Based catalysts under mild conditions, *JACS Au* 1 (2021) 8–12, <https://doi.org/10.1021/jacsau.0c00041>.

- [2] R. Geyer, J.R. Jambeck, K.L. Law, Production, use, and fate of all plastics ever made, *Sci. Adv.* 3 (2017) e1700782, <https://doi.org/10.1126/sciadv.1700782>.
- [3] D.W. Sauter, M. Taoufik, C. Boisson, Polyolefins, a success story, *Polymers* (Basel) 9 (2017), <https://doi.org/10.3390/polym9060185>.
- [4] N. Hassibi, R. Benrabah, Y.A. Vega-Bustos, B. Sirjean, P.-A. Glaude, G. Mauviel, V. Burklé-Vitzthum, Oxidative stability of hydrocarbons produced by pyrolysis of polypropylene, *Fuel* 358 (2024) 130121, <https://doi.org/10.1016/j.fuel.2023.130121>.
- [5] M. Kusenberger, A. Eschenbacher, M.R. Djokic, A. Zayoud, K. Ragaert, S. De Meester, K.M. Van Geem, Opportunities and challenges for the application of post-consumer plastic waste pyrolysis oils as steam cracker feedstocks: to decontaminate or not to decontaminate? *Waste Manag.* 138 (2022) 83–115, <https://doi.org/10.1016/j.wasman.2021.11.009>.
- [6] R.P. Badoni, S.D. Bhagat, G.C. Joshi, Analysis of olefinic hydrocarbons in cracked petroleum stocks: a review, *Fuel* 71 (1992) 483–491, [https://doi.org/10.1016/0016-2361\(92\)90144-D](https://doi.org/10.1016/0016-2361(92)90144-D).
- [7] D.F. de Andrade, D.R. Fernandes, J.L. Miranda, Methods for the determination of conjugated dienes in petroleum products: a review, *Fuel* 89 (2010) 1796–1805, <https://doi.org/10.1016/j.fuel.2010.01.003>.
- [8] D. Zanella, M. Romagnoli, S. Malcangi, M. Beccaria, T. Chenet, C. De Luca, F. Testoni, L. Pasti, U. Visentini, G. Morini, A. Cavazzini, F.A. Franchina, The contribution of high-resolution GC separations in plastic recycling research, *Anal. Bioanal. Chem.* 415 (2023) 2343–2355, <https://doi.org/10.1007/s00216-023-04519-8>.
- [9] H.E. Toraman, T. Dijkmans, M.R. Djokic, K.M. Van Geem, G.B. Marin, Detailed compositional characterization of plastic waste pyrolysis oil by comprehensive two-dimensional gas-chromatography coupled to multiple detectors, *J. Chromatogr. A* 1359 (2014) 237–246, <https://doi.org/10.1016/j.chroma.2014.07.017>.
- [10] M. Auersvald, M. Šiman, P. Vozka, P. Straka, Quantitative determination of olefins in pyrolysis oils from waste plastics and tires using selective adsorption by Ag-SiO₂ followed by GC×GC-FID, *Talanta* 281 (2025) 126792, <https://doi.org/10.1016/j.talanta.2024.126792>.
- [11] H.D. Dubois, D.A. Skoog, Determination of bromine addition numbers, *Anal. Chem.* 20 (1948) 624–627.
- [12] ASTM International, ASTM D1159-23 standard test method for bromine numbers of petroleum distillates and commercial aliphatic olefins by electrometric titration, West Conshohocken, PA, <https://doi.org/10.1520/D1159-23>, 2023.
- [13] M. Auersvald, M. Staš, P. Šimáček, Electrometric bromine number as a suitable method for the quantitative determination of phenols and olefins in hydrotreated pyrolysis bio-oils, *Talanta* 225 (2021) 122001, <https://doi.org/10.1016/j.talanta.2020.122001>.
- [14] J.B. Lewis, R.B. Bradstreet, Determination of unsaturation in aliphatic hydrocarbon mixtures by bromine absorption, *Ind. Eng. Chem. Anal. Ed.* 12 (1940) 387–390.
- [15] M. Auersvald, M. Šiman, E. Lyko Vachková, J. Kroufek, P. Straka, G. Barzallo, P. Vozka, A comparative study of aromatic content in pyrolysis oils from waste plastics and tires: assessing common refinery methods, *Fuel* 369 (2024) 131714, <https://doi.org/10.1016/j.fuel.2024.131714>.
- [16] M. Auersvald, V. Krupka, E.L. Vachková, P. Straka, Determination of olefins in pyrolysis oils from waste plastics and tires – comparability of titration and chromatographic methods, *Fuel* 393 (2025) 134921, <https://doi.org/10.1016/j.fuel.2025.134921>.
- [17] H. Dao Thi, M.R. Djokic, K.M. Van Geem, Detailed group-type characterization of plastic-waste pyrolysis oils: by comprehensive two-dimensional gas chromatography including linear, branched, and Di-Olefins, *Separations* 8 (2021), <https://doi.org/10.3390/separations8070103>.
- [18] D. Frączak, G. Fabiš, B. Orlińska, Influence of the feedstock on the process parameters, product composition and pilot-scale cracking of plastics, *Materials* 14 (2021), <https://doi.org/10.3390/ma14113094>.
- [19] B. Mlynková, M. Bajus, E. Hájeková, G. Kostrab, D. Mravec, Fuels Obtained by Thermal Cracking of Individual and Mixed Polymers, 64, 2010, pp. 15–24, <https://doi.org/10.2478/s11696-009-0102-y>.
- [20] T. Ondrovič, E. Hájeková, J. Mikulec, A. Peller, M. Slezáková, Optimisation of jet fuel production from waste polypropylene in conical reactor, *Petrol. Coal* 66 (2024).
- [21] M.S. Abbas-Abadi, M. Kusenberger, A. Zayoud, M. Roosen, F. Vermeire, S. Madanikashani, M. Kuzmanović, B. Parvizi, U. Kresovic, S. De Meester, K. M. Van Geem, Thermal pyrolysis of waste versus virgin polyolefin feedstocks: the role of pressure, temperature and waste composition, *Waste Manag.* 165 (2023) 108–118, <https://doi.org/10.1016/j.wasman.2023.04.029>.
- [22] J. Mikulec, M. Vrbova, Catalytic and thermal cracking of selected polyolefins, *Clean Technol. Environ. Policy* 10 (2008) 121–130, <https://doi.org/10.1007/s10098-007-0132-5>.
- [23] L. Soják, R. Kubinec, H. Jurdáková, E. Hájeková, M. Bajus, High resolution gas chromatographic-mass spectrometric analysis of polyethylene and polypropylene thermal cracking products, *J. Anal. Appl. Pyrolysis* 78 (2007) 387–399, <https://doi.org/10.1016/j.jaap.2006.09.012>.
- [24] A. Gala, M. Guerrero, B. Guirao, M.E. Domine, J.M. Serra, Characterization and distillation of pyrolysis liquids coming from polyolefins segregated of MSW for their use as automotive diesel fuel, *Energy Fuels* 34 (2020) 5969–5982, <https://doi.org/10.1021/acs.energyfuels.0c00403>.
- [25] M.N. Dunkle, C. Benedetti, P. Pijcke, R. van Belzen, M. Boekwa, M. Mitsios, M. Ruitenbeek, G. Bellos, Comparing different methods for olefin quantification in pygas and plastic pyrolysis oils: gas chromatography-vacuum ultraviolet detection versus comprehensive gas chromatography versus bromine number titration, *J. Chromatogr. A* 1713 (2024) 464569, <https://doi.org/10.1016/j.chroma.2023.464569>.
- [26] ASTM International, ASTM D1492-21 standard test method for bromine index of aromatic hydrocarbons by coulometric titration, West Conshohocken, PA, <https://doi.org/10.1520/D1492-21>, 2021.
- [27] ASTM International, ASTM D2710-20 standard test method for bromine index of petroleum hydrocarbons by electrometric titration, West Conshohocken, PA, <https://doi.org/10.1520/D2710-20>, 2020.
- [28] J.M. Escola, J. Aguado, D.P. Serrano, L. Briones, Transportation fuel production by combination of LDPE thermal cracking and catalytic hydrotreating, *Waste Manag.* 34 (2014) 2176–2184, <https://doi.org/10.1016/j.wasman.2014.06.010>.
- [29] J.M. Escola, D.P. Serrano, J. Aguado, L. Briones, Hydrotreating of the LDPE thermal cracking oil over hierarchical Ni/Beta catalysts with different Ni particle size distributions, *Ind. Eng. Chem. Res.* 54 (2015) 6660–6668, <https://doi.org/10.1021/acs.iecr.5b01160>.
- [30] J.M. Escola, J. Aguado, D.P. Serrano, A. García, A. Peral, L. Briones, R. Calvo, E. Fernandez, Catalytic hydrotreating of the polyethylene thermal cracking oil over Ni supported hierarchical zeolites and mesostructured aluminosilicates, *Appl. Catal., B* 106 (2011) 405–415, <https://doi.org/10.1016/j.apcatb.2011.05.048>.
- [31] J. Walendziewski, Continuous flow cracking of waste plastics, *Fuel Process. Technol.* 86 (2005) 1265–1278, <https://doi.org/10.1016/j.fuproc.2004.12.004>.
- [32] C. Debek, J. Walendziewski, Hydrotreating of oil from pyrolysis of whole tyres for passenger cars and vans, *Fuel* 159 (2015) 659–665, <https://doi.org/10.1016/j.fuel.2015.07.024>.
- [33] A. von Hübl, Eine allgemein anwendbare Methode zur Untersuchung der Fette, *Dingler's Polytech. J.* 253 (1884) 281–295.
- [34] J. Hanus, Die anwendung von jodmonobromid bei der analyse von Fetten und Oelen, *Zeitschrift Für Untersuchung Der Nahrungs-Und Genußmittel, Sowie Der Gebrauchsgegenstände* 4 (1901) 913–920.
- [35] J.J.A. Wijs, Zur Hübl'schen Jodadditionsmethode, *Angew. Chem.* 11 (1898) 291–297.
- [36] International A, ASTM D5554-15 Standard Test Method for Determination of the Iodine Value of Fats and Oils, ASTM International, West Conshohocken, PA, 2021.
- [37] E.H. Unger, Influence of olefin structure on bromine number as determined by various analytical methods, *Anal. Chem.* 30 (1958) 375–380.
- [38] H.D. Hoffman, C.E. Green, A rapid method for the determination of iodine number, *Oil Soap* 16 (1939) 236–238.
- [39] P. Straka, M. Auersvald, D. Vrtiška, H. Kittel, P. Šimáček, P. Vozka, Production of transportation fuels via hydrotreating of scrap tires pyrolysis oil, *Chem. Eng. J.* 460 (2023) 141764, <https://doi.org/10.1016/j.cej.2023.141764>.
- [40] A. Khaleque, M.R. Islam, M.S. Hossain, M. Khan, M.S. Rahman, H. Haniu, Upgrading of waste tyre pyrolysis oil to be used in diesel engine, *Mech. Eng. Res. J* 10 (2016) 35–40.
- [41] N. Jantaraksa, P. Prasassarakich, P. Reubroycharoen, N. Hinchiranan, Cleaner alternative liquid fuels derived from the hydrodesulfurization of waste tire pyrolysis oil, *Energy Convers. Manag.* 95 (2015) 424–434.
- [42] K. Hrynshyn, V. Skorokhoda, T. Chervinskyy, Study on the composition and properties of pyrolysis pyrocondensate of used tires, *Methods* 341 (2022) 314.
- [43] T. Kruatian, K. Jitmanee, Greener analytical method for determination of iodine number of edible oils, *J. Food Res.* 9 (2021) 1–36.
- [44] M. Tubino, J.A. Aricetti, A green potentiometric method for the determination of the iodine number of biodiesel, *Fuel* 103 (2013) 1158–1163, <https://doi.org/10.1016/j.fuel.2012.10.011>.
- [45] U. Dwivedi, K.K. Pant, S.N. Naik, Controlling liquid hydrocarbon composition in valorization of plastic waste via tuning zeolite framework and SiO₂/Al₂O₃ ratio, *J. Environ. Manag.* 297 (2021) 113288, <https://doi.org/10.1016/j.jenvman.2021.113288>.
- [46] B.K. Sharma, B.R. Moser, K.E. Vermillion, K.M. Doll, N. Rajagopalan, Production, characterization and fuel properties of alternative diesel fuel from pyrolysis of waste plastic grocery bags, *Fuel Process. Technol.* 122 (2014) 79–90, <https://doi.org/10.1016/j.fuproc.2014.01.019>.
- [47] J.S. dos Passos, C. Lorentz, D. Laurenti, S.-J. Royer, I. Chontzoglou, P. Biller, Hydrothermal liquefaction of plastic marine debris from the north Pacific garbage patch, *Resour. Conserv. Recycl.* 209 (2024) 107822, <https://doi.org/10.1016/j.resconrec.2024.107822>.
- [48] X. Jing, G. Yan, Y. Zhao, H. Wen, Z. Xu, Study on mild cracking of polyolefins to liquid hydrocarbons in a closed batch reactor for subsequent olefin recovery, *Polym. Degrad. Stabil.* 109 (2014) 79–91, <https://doi.org/10.1016/j.polymdegradstab.2014.07.003>.
- [49] X. Jing, Y. Zhao, H. Wen, Z. Xu, Interactions between low-density polyethylene (LDPE) and polypropylene (PP) during the mild cracking of polyolefin mixtures in a closed-batch reactor, *Energy Fuels* 27 (2013) 5841–5851, <https://doi.org/10.1021/ef401376m>.
- [50] M. Rezaei, R. Gieleciak, K.H. Michaelian, Determination of olefin contents in liquid hydrocarbons using a quantum Cascade laser and a photoacoustic detector, *Energy Fuels* 33 (2019) 2859–2866, <https://doi.org/10.1021/acs.energyfuels.8b03760>.
- [51] G. Yan, X. Jing, H. Wen, S. Xiang, Thermal cracking of virgin and waste plastics of PP and LDPE in a semibatch reactor under atmospheric pressure, *Energy Fuels* 29 (2015) 2289–2298, <https://doi.org/10.1021/ef502919f>.
- [52] A. Sinağ, M. Sungur, M. Güllü, M. Canel, Characterization of the liquid phase obtained by copyrolysis of mustafa kemal paşa (M.K.P.) lignite (Turkey) with low density polyethylene, *Energy Fuels* 20 (2006) 2093–2098, <https://doi.org/10.1021/ef060213v>.

- [53] G.R. Saha, T. Das, P. Handique, D. Kalita, B.K. Saikia, Copyrolysis of low-grade Indian coal and waste plastics: future prospects of waste plastic as a source of fuel, *Energy Fuels* 32 (2018) 2421–2431, <https://doi.org/10.1021/acs.energyfuels.7b03298>.
- [54] R. Gieleciak, A. Hall, K. Michaelian, J. Chen, Exploring the potential of raman spectroscopy for characterizing olefins in olefin-containing streams, *Energy Fuels* 37 (2023) 13698–13709, <https://doi.org/10.1021/acs.energyfuels.3c02014>.
- [55] A.Kh. Kuptsov, E. V. Zhmaeva, A. V. Kulik, K.B. Rudyak, Laser raman spectroscopy – an effective method for total process control of Poly- α -Olefin oil production, *Chem. Technol. Fuels Oils* 58 (2022) 772–778, <https://doi.org/10.1007/s10553-022-01449-6>.
- [56] J.J. Heigl, J.F. Black, B.F. Dudenbostel Jr., Determination of total olefins and total aromatics, *Anal. Chem.* 21 (1949) 554–559.
- [57] A. Gopanna, R.N. Mandapati, S.P. Thomas, K. Rajan, M. Chavali, Fourier transform infrared spectroscopy (FTIR), Raman spectroscopy and wide-angle X-ray scattering (WAXS) of polypropylene (PP)/cyclic olefin copolymer (COC) blends for qualitative and quantitative analysis, *Polym. Bull.* 76 (2019) 4259–4274, <https://doi.org/10.1007/s00289-018-2599-0>.
- [58] M.E. Myers, Janis Stollsteimer, A.M. Wims, Determination of gasoline octane numbers from chemical composition, *Anal. Chem.* 47 (1975) 2301–2304, <https://doi.org/10.1021/ac60363a015>.
- [59] 96/05665 gasoline analysis by ^1H nuclear magnetic resonance spectroscopy, *Fuel Energy Abstr.* 37 (1996) 391, [https://doi.org/10.1016/0140-6701\(96\)80315-8](https://doi.org/10.1016/0140-6701(96)80315-8).
- [60] U. Kumar, V. Gaikwad, M. Mayyas, M. Bucknall, V. Sahajwalla, Application of high-resolution NMR and GC–MS to study hydrocarbon oils derived from noncatalytic thermal transformation of e-Waste plastics, *ACS Omega* 3 (2018) 9282–9289, <https://doi.org/10.1021/acsomega.8b01284>.
- [61] A. International, ASTM D1319-20a Standard Test Method for Hydrocarbon Types in Liquid Petroleum Products by Fluorescent Indicator Adsorption, 2020.
- [62] G. Barzallo, H. Gieng, E.N. Luu, M. Auersvald, P. Straka, P. Vozka, Quantitative analysis of aliphatic olefins in alternative and petroleum-based fuels by comprehensive two-dimensional gas chromatography, in: *ACS Fall*, 2022.
- [63] B.N. Barman, V.L. Cebolla, L. Membrado, Chromatographic techniques for petroleum and related products, *Crit. Rev. Anal. Chem.* 30 (2000) 75–120, <https://doi.org/10.1080/10408340091164199>.
- [64] B.P. Vempatapu, J. Kumar, B. Upreti, P.K. Kanaujia, Application of high-performance liquid chromatography in petroleum analysis: challenges and opportunities, *TrAC, Trends Anal. Chem.* 177 (2024) 117810, <https://doi.org/10.1016/j.trac.2024.117810>.
- [65] J.C. Suatoni, R.E. Swab, HPLC preparative group-type separation of olefins from synfuels, *J. Chromatogr. Sci.* 18 (1980) 375–378, <https://doi.org/10.1093/chromsci/18.8.375>.
- [66] K. Jinno, H. Nomura, Y. Hirata, Group-type analysis of gasoline range materials by high performance liquid chromatography, *J. High Resolut. Chromatogr.* 3 (1980) 503–506, <https://doi.org/10.1002/jhrc.1240031004>.
- [67] A. Yadav, V. Kagdiyal, A. Arun, M.B. Patel, A.A. Gupta, B. Basu, HPLC method for monitoring the conjugated dienes and olefins in FCC, coker gasolines, and their hydrogenated products, *J. Liq. Chromatogr. Relat. Technol.* 38 (2015) 840–846, <https://doi.org/10.1080/10826076.2014.968663>.
- [68] A. Yadav, K. Chattopadhyay, R. Singh, S. Mondal, A. Chopra, J. Christopher, G. S. Kapur, Novel HPLC-RI-UV based method for simultaneous estimation of saturates, olefins, conjugated dienes and aromatics in full range cracked gasoline, *Petrol. Sci. Technol.* 36 (2018) 1805–1811, <https://doi.org/10.1080/10916466.2018.1511597>.
- [69] Jasco, Evaluation of the SFC-FID for the Olefin Analysis ASTM D6550 Method, 2020. Easton, MD.
- [70] A.S. Kaplitz, S. Marshall, N. Bhakta, S. Morshed, J.-F. Borny, K.A. Schug, Discrimination of plastic waste pyrolysis oil feedstocks using supercritical fluid chromatography, *J. Chromatogr. A* 1720 (2024) 464804, <https://doi.org/10.1016/j.chroma.2024.464804>.
- [71] R. Firor, Fast Refinery Gas Analysis System Based on the Agilent 7890B GC System and G3507A Large Valve Oven Using Micropacked Columns, 2013.
- [72] M. Artetxe, G. Lopez, G. Elordi, M. Amutio, J. Bilbao, M. Olazar, Production of light olefins from polyethylene in a two-step process: pyrolysis in a conical spouted bed and downstream high-temperature thermal cracking, *Ind. Eng. Chem. Res.* 51 (2012) 13915–13923, <https://doi.org/10.1021/ie300178e>.
- [73] M. Artetxe, G. Lopez, M. Amutio, G. Elordi, J. Bilbao, M. Olazar, Cracking of high density polyethylene pyrolysis waxes on HZSM-5 catalysts of different acidity, *Ind. Eng. Chem. Res.* 52 (2013) 10637–10645, <https://doi.org/10.1021/ie4014869>.
- [74] S. Orozco, M. Artetxe, G. Lopez, M. Suarez, J. Bilbao, M. Olazar, Conversion of HDPE into value products by fast pyrolysis using FCC spent catalysts in a fountain confined conical spouted bed reactor, *ChemSusChem* 14 (2021) 4291–4300, <https://doi.org/10.1002/cssc.202100889>.
- [75] J. Zeaiter, A process study on the pyrolysis of waste polyethylene, *Fuel* 133 (2014) 276–282, <https://doi.org/10.1016/j.fuel.2014.05.028>.
- [76] D.S. Achilias, C. Roupakias, P. Megalokonomos, A.A. Lappas, E. V. Antonakou, Chemical recycling of plastic wastes made from polyethylene (LDPE and HDPE) and polypropylene (PP), *J. Hazard Mater.* 149 (2007) 536–542, <https://doi.org/10.1016/j.jhazmat.2007.06.076>.
- [77] Y. Zhang, G. Ji, C. Chen, Y. Wang, W. Wang, A. Li, Liquid oils produced from pyrolysis of plastic wastes with heat carrier in rotary kiln, *Fuel Process. Technol.* 206 (2020) 106455, <https://doi.org/10.1016/j.fuproc.2020.106455>.
- [78] P. Das, P. Tiwari, Valorization of packaging plastic waste by slow pyrolysis, *Resour. Conserv. Recycl.* 128 (2018) 69–77, <https://doi.org/10.1016/j.resconrec.2017.09.025>.
- [79] P. Das, P. Tiwari, The effect of slow pyrolysis on the conversion of packaging waste plastics (PE and PP) into fuel, *Waste Manag.* 79 (2018) 615–624, <https://doi.org/10.1016/j.wasman.2018.08.021>.
- [80] Y. Jaafar, L. Abdelouahed, R. El Hage, A. El Samrani, B. Taouk, Pyrolysis of common plastics and their mixtures to produce valuable petroleum-like products, *Polym. Degrad. Stabil.* 195 (2022) 109770, <https://doi.org/10.1016/j.polymerdegradstab.2021.109770>.
- [81] A. López, I. de Marco, B.M. Caballero, M.F. Laresgoiti, A. Adrados, Influence of time and temperature on pyrolysis of plastic wastes in a semi-batch reactor, *Chem. Eng. J.* 173 (2011) 62–71, <https://doi.org/10.1016/j.cej.2011.07.037>.
- [82] F. Obeid, J. Zeaiter, A.H. Al-Muhtaseb, K. Bouhadir, Thermo-catalytic pyrolysis of waste polyethylene bottles in a packed bed reactor with different bed materials and catalysts, *Energy Convers. Manag.* 85 (2014) 1–6, <https://doi.org/10.1016/j.enconman.2014.05.075>.
- [83] K.M. Van Geem, S.P. Pyl, M.-F. Reyniers, J. Vercammen, J. Beens, G.B. Marin, On-line analysis of complex hydrocarbon mixtures using comprehensive two-dimensional gas chromatography, *J. Chromatogr. A* 1217 (2010) 6623–6633, <https://doi.org/10.1016/j.chroma.2010.04.006>.
- [84] G. Yan, X. Jing, H. Wen, S. Xiang, Thermal cracking of virgin and waste plastics of PP and LDPE in a semibatch reactor under atmospheric pressure, *Energy Fuels* 29 (2015) 2289–2298, <https://doi.org/10.1021/ef502919f>.
- [85] Y. Wang, K. Wu, Q. Liu, H. Zhang, Low chlorine oil production through fast pyrolysis of mixed plastics combined with hydrothermal dechlorination pretreatment, *Process Saf. Environ. Prot.* 149 (2021) 105–114, <https://doi.org/10.1016/j.psep.2020.10.023>.
- [86] Z. Dobó, G. Kecsmár, G. Nagy, T. Koós, G. Muránszky, M. Ayari, Characterization of gasoline-like transportation fuels obtained by distillation of pyrolysis oils from plastic waste mixtures, *Energy Fuels* 35 (2021) 2347–2356, <https://doi.org/10.1021/acs.energyfuels.0c04022>.
- [87] N. Miskolczi, L. Bartha, A. Angyal, Pyrolysis of polyvinyl chloride (PVC)-containing mixed plastic wastes for recovery of hydrocarbons, *Energy Fuels* 23 (2009) 2743–2749, <https://doi.org/10.1021/ef8011245>.
- [88] N. Miskolczi, L. Bartha, G. Deák, B. Jóver, Thermal degradation of municipal plastic waste for production of fuel-like hydrocarbons, *Polym. Degrad. Stabil.* 86 (2004) 357–366, <https://doi.org/10.1016/j.polymerdegradstab.2004.04.025>.
- [89] A. Zayoud, H. Dao Thi, M. Kusenberger, A. Eschenbacher, U. Kresovic, N. Alderweireldt, M. Djokic, K.M. Van Geem, Pyrolysis of end-of-life polystyrene in a pilot-scale reactor: maximizing styrene production, *Waste Manag.* 139 (2022) 85–95, <https://doi.org/10.1016/j.wasman.2021.12.018>.
- [90] H.-T. Lin, M.-S. Huang, J.-W. Luo, L.-H. Lin, C.-M. Lee, K.-L. Ou, Hydrocarbon fuels produced by catalytic pyrolysis of hospital plastic wastes in a fluidizing cracking process, *Fuel Process. Technol.* 91 (2010) 1355–1363, <https://doi.org/10.1016/j.fuproc.2010.03.016>.
- [91] N. Miskolczi, A. Angyal, L. Bartha, I. Valkai, Fuels by pyrolysis of waste plastics from agricultural and packaging sectors in a pilot scale reactor, *Fuel Process. Technol.* 90 (2009) 1032–1040, <https://doi.org/10.1016/j.fuproc.2009.04.019>.
- [92] P. Lovás, P. Hudec, B. Jambor, E. Hájeková, M. Hornáček, Catalytic cracking of heavy fractions from the pyrolysis of waste HDPE and, *Fuel* 203 (2017) 244–252, <https://doi.org/10.1016/j.fuel.2017.04.128>.
- [93] L. Ballice, Classification of volatile products evolved during temperature-programmed co-pyrolysis of low-density polyethylene (LDPE) with polypropylene (PP), *Fuel* 81 (2002) 1233–1240, [https://doi.org/10.1016/S0016-2361\(01\)00130-2](https://doi.org/10.1016/S0016-2361(01)00130-2).
- [94] L. Ballice, M. Yüksel, M. Sağlam, R. Reimert, H. Schulz, Classification of volatile products from the temperature-programmed pyrolysis of Low- and high-density polyethylene, *Energy Fuels* 12 (1998) 925–928, <https://doi.org/10.1021/ef980004d>.
- [95] G. Elordi, M. Olazar, G. Lopez, M. Artetxe, J. Bilbao, Product yields and compositions in the continuous pyrolysis of high-density polyethylene in a conical spouted bed reactor, *Ind. Eng. Chem. Res.* 50 (2011) 6650–6659, <https://doi.org/10.1021/ie200186m>.
- [96] W. Kaminsky, B. Schlesselmann, C. Simon, Olefins from polyolefins and mixed plastics by pyrolysis, *J. Anal. Appl. Pyrolysis* 32 (1995) 19–27, [https://doi.org/10.1016/0165-2370\(94\)00830-T](https://doi.org/10.1016/0165-2370(94)00830-T).
- [97] J.A. Onwudili, N. Insura, P.T. Williams, Composition of products from the pyrolysis of polyethylene and polystyrene in a closed batch reactor: effects of temperature and residence time, *J. Anal. Appl. Pyrolysis* 86 (2009) 293–303, <https://doi.org/10.1016/j.jaap.2009.07.008>.
- [98] M. del Remedio Hernández, A.N. García, A. Marcilla, Catalytic flash pyrolysis of HDPE in a fluidized bed reactor for recovery of fuel-like hydrocarbons, *J. Anal. Appl. Pyrolysis* 78 (2007) 272–281, <https://doi.org/10.1016/j.jaap.2006.03.009>.
- [99] A. Marcilla, M.I. Beltrán, R. Navarro, Thermal and catalytic pyrolysis of polyethylene over HZSM5 and HUSY zeolites in a batch reactor under dynamic conditions, *Appl. Catal., B* 86 (2009) 78–86, <https://doi.org/10.1016/j.apcatb.2008.07.026>.
- [100] R. van Grieken, D.P. Serrano, J. Aguado, R. García, C. Rojo, Thermal and catalytic cracking of polyethylene under mild conditions, *J. Anal. Appl. Pyrolysis* 58–59 (2001) 127–142, [https://doi.org/10.1016/S0165-2370\(00\)00145-5](https://doi.org/10.1016/S0165-2370(00)00145-5).
- [101] P.N. Sharratt, Y.-H. Lin, A.A. Garforth, J. Dwyer, Investigation of the catalytic pyrolysis of high-density polyethylene over a HZSM-5 catalyst in a laboratory fluidized-bed reactor, *Ind. Eng. Chem. Res.* 36 (1997) 5118–5124, <https://doi.org/10.1021/ie970348b>.
- [102] A. Eschenbacher, R.J. Varghese, M.S. Abbas-Abadi, K.M. Van Geem, Maximizing light olefins and aromatics as high value base chemicals via single step catalytic conversion of plastic waste, *Chem. Eng. J.* 428 (2022) 132087, <https://doi.org/10.1016/j.cej.2021.132087>.

- [103] A. Eschenbacher, F. Goodarzi, R.J. Varghese, K. Enemark-Rasmussen, S. Kegnes, M.S. Abbas-Abadi, K.M. Van Geem, Boron-modified mesoporous ZSM-5 for the conversion of pyrolysis vapors from LDPE and mixed polyolefins: maximizing the C2–C4 olefin yield with minimal carbon footprint, *ACS Sustain. Chem. Eng.* 9 (2021) 14618–14630, <https://doi.org/10.1021/acssuschemeng.1c06098>.
- [104] RESTEK, PIONA Calibration standard on Rtx-DHA-100 by ASTM D6729-14, <https://www.restek.com/Chromatogram-Detail/GC.PC1330> (n.d.).
- [105] M.N. Dunkle, P. Pijcke, B. Winniford, G. Bellos, Quantification of the composition of liquid hydrocarbon streams: comparing the GC-VUV to DHA and GCxGC, *J. Chromatogr. A* 1587 (2019) 239–246, <https://doi.org/10.1016/j.chroma.2018.12.026>.
- [106] Y.-H. Seo, D.-H. Shin, Determination of paraffin and aromatic hydrocarbon type chemicals in liquid distillates produced from the pyrolysis process of waste plastics by isotope-dilution mass spectrometry, *Fuel* 81 (2002) 2103–2112, [https://doi.org/10.1016/S0016-2361\(02\)00197-7](https://doi.org/10.1016/S0016-2361(02)00197-7).
- [107] P.T. Williams, E. Slaney, Analysis of products from the pyrolysis and liquefaction of single plastics and waste plastic mixtures, *Resour. Conserv. Recycl.* 51 (2007) 754–769, <https://doi.org/10.1016/j.resconrec.2006.12.002>.
- [108] K.-H. Lee, D.-H. Shin, Characteristics of liquid product from the pyrolysis of waste plastic mixture at low and high temperatures: influence of lapse time of reaction, *Waste Manag.* 27 (2007) 168–176, <https://doi.org/10.1016/j.wasman.2005.12.017>.
- [109] W. Jeon, Y.-D. Kim, K.-H. Lee, A comparative study on pyrolysis of bundle and fluffy shapes of waste packaging plastics, *Fuel* 283 (2021) 119260, <https://doi.org/10.1016/j.fuel.2020.119260>.
- [110] L. Cheng, J. Gu, Y. Wang, J. Zhang, H. Yuan, Y. Chen, Polyethylene high-pressure pyrolysis: better product distribution and process mechanism analysis, *Chem. Eng. J.* 385 (2020) 123866, <https://doi.org/10.1016/j.cej.2019.123866>.
- [111] E. Hájeková, M. Bajus, Recycling of low-density polyethylene and polypropylene via copyrolysis of polyalkene oil/waxes with naphtha: product distribution and coke formation, *J. Anal. Appl. Pyrolysis* 74 (2005) 270–281, <https://doi.org/10.1016/j.jaap.2004.11.016>.
- [112] D. Lee, H. Nam, S. Wang, H. Kim, J.H. Kim, Y. Won, B.W. Hwang, Y.D. Kim, H. Nam, K.-H. Lee, H.-J. Ryu, Characteristics of fractionated drop-in liquid fuel of plastic wastes from a commercial pyrolysis plant, *Waste Manag.* 126 (2021) 411–422, <https://doi.org/10.1016/j.wasman.2021.03.020>.
- [113] R. Miandad, M. Rehan, M.A. Barakat, A.S. Aburizaiza, H. Khan, I.M.I. Ismail, J. Dhavamani, J. Gardy, A. Hassanpour, A.-S. Nizami, Catalytic pyrolysis of plastic waste: moving toward pyrolysis based biorefineries, *Front. Energy Res.* 7 (2019) 437000.
- [114] L. Quesada, M. Calero, M.Á. Martín-Lara, A. Pérez, G. Blázquez, Production of an alternative fuel by pyrolysis of plastic wastes mixtures, *Energy Fuels* 34 (2020) 1781–1790, <https://doi.org/10.1021/acs.energyfuels.9b03350>.
- [115] I. Ahmad, M.I. Khan, H. Khan, M. Ishaq, R. Tariq, K. Gul, W. Ahmad, Pyrolysis study of polypropylene and polyethylene into premium oil products, *Int. J. Green Energy* 12 (2015) 663–671, <https://doi.org/10.1080/15435075.2014.880146>.
- [116] S. Wang, H. Kim, D. Lee, Y.-R. Lee, Y. Won, B.W. Hwang, H. Nam, H.-J. Ryu, K.-H. Lee, Drop-in fuel production with plastic waste pyrolysis oil over catalytic separation, *Fuel* 305 (2021) 121440, <https://doi.org/10.1016/j.fuel.2021.121440>.
- [117] T. Ueno, E. Nakashima, K. Takeda, Quantitative analysis of random scission and chain-end scission in the thermal degradation of polyethylene, *Polym. Degrad. Stabil.* 95 (2010) 1862–1869, <https://doi.org/10.1016/j.polymerdegradstab.2010.04.020>.
- [118] A. Demirbas, O. Taylan, Recovery of gasoline-range hydrocarbons from petroleum basic plastic wastes, *Petrol. Sci. Technol.* 33 (2015) 1883–1889, <https://doi.org/10.1080/10916466.2015.1110594>.
- [119] C. Berruero, F.J. Mastral, E. Esperanza, J. Ceamanos, Production of waxes and tars from the continuous pyrolysis of high density polyethylene. Influence of operation variables, *Energy Fuels* 16 (2002) 1148–1153, <https://doi.org/10.1021/ef020008p>.
- [120] R.K. Singh, B. Ruj, A.K. Sadhukhan, P. Gupta, Impact of fast and slow pyrolysis on the degradation of mixed plastic waste: product yield analysis and their characterization, *J. Energy Inst.* 92 (2019) 1647–1657, <https://doi.org/10.1016/j.joei.2019.01.009>.
- [121] M. Staš, M. Auersvald, L. Kejla, D. Vrtiška, J. Kroufek, D. Kubička, Quantitative analysis of pyrolysis bio-oils: a review, *TrAC, Trends Anal. Chem.* 126 (2020) 115857, <https://doi.org/10.1016/j.trac.2020.115857>.
- [122] Y.-H. Seo, K.-H. Lee, D.-H. Shin, Investigation of catalytic degradation of high-density polyethylene by hydrocarbon group type analysis, *J. Anal. Appl. Pyrolysis* 70 (2003) 383–398, [https://doi.org/10.1016/S0165-2370\(02\)00186-9](https://doi.org/10.1016/S0165-2370(02)00186-9).
- [123] K.-H. Lee, Pyrolysis of municipal plastic wastes separated by difference of specific gravity, *J. Anal. Appl. Pyrolysis* 79 (2007) 362–367, <https://doi.org/10.1016/j.jaap.2006.12.020>.
- [124] K.-H. Lee, S.-G. Jeon, K.-H. Kim, N.-S. Noh, D.-H. Shin, J. Park, Y. Seo, J.-J. Yee, G.-T. Kim, Thermal and catalytic degradation of waste high-density polyethylene (HDPE) using spent FCC catalyst, *Kor. J. Chem. Eng.* 20 (2003) 693–697, <https://doi.org/10.1007/BF02706909>.
- [125] A. Serras-Maillols, B.B. Perez-Martinez, A. Iriondo, E. Acha, A. Lopez-Uribebarrenechea, B.M. Caballero, Quantification of the composition of pyrolysis oils of complex plastic waste by gas chromatography coupled with mass spectrometer detector, *RSC Adv.* 14 (2024) 9892–9911.
- [126] K. Schofield, The enigmatic mechanism of the flame ionization detector: its overlooked implications for fossil fuel combustion modeling, *Prog. Energy Combust. Sci.* 34 (2008) 330–350, <https://doi.org/10.1016/j.pecs.2007.08.001>.
- [127] J.T. Scanlon, D.E. Willis, Calculation of flame ionization detector relative response factors using the effective carbon number concept, *J. Chromatogr. Sci.* 23 (1985) 333–340.
- [128] D.P. Serrano, J. Aguado, J.M. Escola, E. Garagorri, Performance of a continuous screw kiln reactor for the thermal and catalytic conversion of polyethylene–lubricating oil base mixtures, *Appl. Catal., B* 44 (2003) 95–105, [https://doi.org/10.1016/S0926-3373\(03\)00024-9](https://doi.org/10.1016/S0926-3373(03)00024-9).
- [129] S.H. Ng, H. Seoud, M. Stanculescu, Y. Sugimoto, Conversion of polyethylene to transportation fuels through pyrolysis and catalytic cracking, *Energy Fuels* 9 (1995) 735–742, <https://doi.org/10.1021/ef00053a002>.
- [130] S. Ucar, S. Karagoz, A.R. Ozkan, J. Yanik, Evaluation of two different scrap tires as hydrocarbon source by pyrolysis, *Fuel* 84 (2005) 1884–1892, <https://doi.org/10.1016/j.fuel.2005.04.002>.
- [131] F. Campuzano, A.G. Abdul Jameel, W. Zhang, A.-H. Emwas, A.F. Agudelo, J. D. Martinez, S.M. Sarathy, On the distillation of waste tire pyrolysis oil: a structural characterization of the derived fractions, *Fuel* 290 (2021) 120041, <https://doi.org/10.1016/j.fuel.2020.120041>.
- [132] R. Miandad, M.A. Barakat, A.S. Aburizaiza, M. Rehan, I.M.I. Ismail, A.S. Nizami, Effect of plastic waste types on pyrolysis liquid oil, *Int. Biodeterior. Biodegrad.* 119 (2017) 239–252, <https://doi.org/10.1016/j.ibiod.2016.09.017>.
- [133] L. Ballice, A kinetic approach to the temperature-programmed pyrolysis of low- and high-density polyethylene in a fixed bed reactor: determination of kinetic parameters for the evolution of n-paraffins and 1-olefins, *Fuel* 80 (2001) 1923–1935, [https://doi.org/10.1016/S0016-2361\(01\)00067-9](https://doi.org/10.1016/S0016-2361(01)00067-9).
- [134] E. Hájeková, L. Špodová, M. Bajus, B. Mlynková, Separation and Characterization of Products from Thermal Cracking of Individual and Mixed Polyalkenes, 61, 2007, pp. 262–270, <https://doi.org/10.2478/s11696-007-0031-6>.
- [135] B. Fekhar, L. Gombor, N. Miskolczi, Pyrolysis of chlorine contaminated municipal plastic waste: in-situ upgrading of pyrolysis oils by Ni/ZSM-5, Ni/SAP-11, red mud and Ca(OH)₂ containing catalysts, *J. Energy Inst.* 92 (2019) 1270–1283, <https://doi.org/10.1016/j.joei.2018.10.007>.
- [136] U. Hujuri, A.K. Ghoshal, S. Gumma, Temperature-dependent pyrolytic product evolution profile for low-density polyethylene from gas chromatographic study, *Waste Manag.* 30 (2010) 814–820, <https://doi.org/10.1016/j.wasman.2009.12.013>.
- [137] M.N. Dunkle, P. Pijcke, W.L. Winniford, M. Ruitenbeek, G. Bellos, Method development and evaluation of pyrolysis oils from mixed waste plastic by GC-VUV, *J. Chromatogr. A* 1637 (2021) 461837, <https://doi.org/10.1016/j.chroma.2020.461837>.
- [138] M. Roosen, L. Harinck, S. Ügdüler, T. De Somer, A.-G. Hucks, T.G.A. Belé, A. Buettner, K. Ragaert, K.M. Van Geem, A. Dumoulin, S. De Meester, Deodorization of post-consumer plastic waste fractions: a comparison of different washing media, *Sci. Total Environ.* 812 (2022) 152467, <https://doi.org/10.1016/j.scitotenv.2021.152467>.
- [139] M. Roosen, M. Mys, M. Kusenber, P. Billen, A. Dumoulin, J. Dewulf, K.M. Van Geem, K. Ragaert, S. De Meester, Detailed analysis of the composition of selected plastic packaging waste products and its implications for mechanical and thermochemical recycling, *Environ. Sci. Technol.* 54 (2020) 13282–13293, <https://doi.org/10.1021/acs.est.0c03371>.
- [140] M.S. Abbas-Abadi, A. Zayoud, M. Kusenber, M. Roosen, F. Vermeire, P. Yazdani, J. Van Waeyenberg, A. Eschenbacher, F.J.A. Hernandez, M. Kuzmanović, H. Dao Thi, U. Kresovic, B. Sels, P. Van Puyvelde, S. De Meester, M. Saeys, K.M. Van Geem, Thermochemical recycling of end-of-life and virgin HDPE: a pilot-scale study, *J. Anal. Appl. Pyrolysis* 166 (2022) 105614, <https://doi.org/10.1016/j.jaap.2022.105614>.
- [141] O. Akin, Q. He, P. Yazdani, Y. Wang, R.J. Varghese, H. Poelman, P. Van Steenberg, K.M. Van Geem, Tailored HZSM-5 catalyst modification via phosphorus impregnation and mesopore introduction for selective catalytic conversion of polypropylene into light olefins, *J. Anal. Appl. Pyrolysis* 181 (2024) 106592, <https://doi.org/10.1016/j.jaap.2024.106592>.
- [142] M. Kusenber, M. Roosen, A. Zayoud, M.R. Djokic, H. Dao Thi, S. De Meester, K. Ragaert, U. Kresovic, K.M. Van Geem, Assessing the feasibility of chemical recycling via steam cracking of untreated plastic waste pyrolysis oils: feedstock impurities, product yields and coke formation, *Waste Manag.* 141 (2022) 104–114, <https://doi.org/10.1016/j.wasman.2022.01.033>.
- [143] M. Kusenber, A. Zayoud, M. Roosen, H.D. Thi, M.S. Abbas-Abadi, A. Eschenbacher, U. Kresovic, S. De Meester, K.M. Van Geem, A comprehensive experimental investigation of plastic waste pyrolysis oil quality and its dependence on the plastic waste composition, *Fuel Process. Technol.* 227 (2022) 107090, <https://doi.org/10.1016/j.fuproc.2021.107090>.
- [144] M. Kusenber, M. Roosen, A. Doktor, L. Casado, A. Jamil Abdulrahman, B. Parvizi, A. Eschenbacher, E. Biadi, N. Laudou, D. Jänsch, S. De Meester, K. M. Van Geem, Contaminant removal from plastic waste pyrolysis oil via depth filtration and the impact on chemical recycling: a simple solution with significant impact, *Chem. Eng. J.* 473 (2023) 145259, <https://doi.org/10.1016/j.cej.2023.145259>.
- [145] M. Kusenber, G.C. Faussone, H.D. Thi, M. Roosen, M. Grilc, A. Eschenbacher, S. De Meester, K.M. Van Geem, Maximizing olefin production via steam cracking of distilled pyrolysis oils from difficult-to-recycle municipal plastic waste and marine litter, *Sci. Total Environ.* 838 (2022) 156092, <https://doi.org/10.1016/j.scitotenv.2022.156092>.
- [146] K. Jin, P. Vozka, C. Gentilcore, G. Kilaz, N.-H.L. Wang, Low-pressure hydrothermal processing of mixed polyolefin wastes into clean fuels, *Fuel* 294 (2021) 120505, <https://doi.org/10.1016/j.fuel.2021.120505>.

- [147] K. Jin, P. Vozka, G. Kilaz, W.-T. Chen, N.-H.L. Wang, Conversion of polyethylene waste into clean fuels and waxes via hydrothermal processing (HTP), *Fuel* 273 (2020) 117726, <https://doi.org/10.1016/j.fuel.2020.117726>.
- [148] C. Un, C. Gentilcore, K. Ault, H. Gieng, P. Vozka, N.-H.L. Wang, Low-pressure hydrothermal processing of disposable face masks into oils, *Processes* 11 (2023) 2819.
- [149] B.A. Perez, H.E. Toraman, Investigating primary decomposition of polypropylene through detailed compositional analysis using two-dimensional gas chromatography and principal component analysis, *J. Anal. Appl. Pyrolysis* 177 (2024) 106376, <https://doi.org/10.1016/j.jaap.2024.106376>.
- [150] J. Wu, Z. Jiang, V.S. Cecon, G. Curtzwiler, K. Vorst, M. Mavrikakis, G.W. Huber, The effects of polyolefin structure and source on pyrolysis-derived plastic oil composition, *Green Chem.* 26 (2024) 11908–11923, <https://doi.org/10.1039/D4GC04029E>.
- [151] Y. Ureel, M.L. Chacón-Patiño, M. Kusenberg, A. Ginzburg, R.P. Rodgers, M. K. Sabbe, K.M. Van Geem, Compositional analysis of oxygenates and hydrocarbons in waste and virgin polyolefin pyrolysis oils by ultrahigh-resolution fourier transform ion cyclotron resonance mass spectrometry, *Energy Fuels* 39 (2025) 1283–1295, <https://doi.org/10.1021/acs.energyfuels.4c03835>.
- [152] K.A. Schug, I. Sawicki, D.D.Jr. Carlton, H. Fan, H.M. McNair, J.P. Nimmo, P. Kroll, J. Smuts, P. Walsh, D. Harrison, Vacuum ultraviolet detector for gas chromatography, *Anal. Chem.* 86 (2014) 8329–8335, <https://doi.org/10.1021/ac5018343>.
- [153] VUV Analytics, Best new analytical instrument. <https://Vuvanalytics.Com/Vuv-Analytics-Awarded-Best-New-Analytical-Instrument-at-the-Gulf-Coast-Conference/>, 2014.
- [154] VUV Analytics, VGA-100, [https://Vuvanalytics.Com/Vga-100-Detector/\(n.d.\)](https://Vuvanalytics.Com/Vga-100-Detector/(n.d.)).
- [155] VUV Analytics, VGA-101, [https://Vuvanalytics.Com/Vga-101-Detector/\(n.d.\)](https://Vuvanalytics.Com/Vga-101-Detector/(n.d.)).
- [156] P. Walsh, M. Garbalena, K.A. Schug, Rapid analysis and time interval deconvolution for comprehensive fuel compound group classification and speciation using gas chromatography–vacuum ultraviolet spectroscopy, *Anal. Chem.* 88 (2016) 11130–11138, <https://doi.org/10.1021/acs.analchem.6b03226>.
- [157] A.S. Kaplitz, K.A. Schug, Gas Chromatography–vacuum ultraviolet spectroscopy in petroleum and fuel analysis, *Analytical Science Advances* 4 (2023) 220–231, <https://doi.org/10.1002/ansa.202300025>.
- [158] D.C. Bell, J. Feldhausen, A.J. Spieles, R.C. Boehm, J.S. Heyne, Limits of identification using VUV spectroscopy applied to C8H18 isomers isolated by GC×GC, *Talanta* 258 (2023) 124451, <https://doi.org/10.1016/j.talanta.2023.124451>.
- [159] Y. Ureel, C.P. Piña, M.N. Dunkle, P. Pijcke, B. da Costa Magalhães, M. Kusenberg, G. Bellos, M.K. Sabbe, J.W. Thybaut, K.M. Van Geem, Detailed analysis of olefins and diolefins in hydrotreated plastic waste pyrolysis oils by GC-VUV, *Waste Manag.* 202 (2025) 114828, <https://doi.org/10.1016/j.wasman.2025.114828>.
- [160] A. Lelevic, V. Souchon, M. Moreaud, C. Lorentz, C. Geantet, Gas chromatography vacuum ultraviolet spectroscopy: a review, *J. Separ. Sci.* 43 (2020) 150–173, <https://doi.org/10.1002/jssc.201900770>.
- [161] L. Bai, J. Smuts, P. Walsh, C. Qiu, H.M. McNair, K.A. Schug, Pseudo-absolute quantitative analysis using gas chromatography – Vacuum ultraviolet spectroscopy – a tutorial, *Anal. Chim. Acta* 953 (2017) 10–22, <https://doi.org/10.1016/j.aca.2016.11.039>.
- [162] A. Lelevic, C. Geantet, C. Lorentz, M. Moreaud, V. Souchon, Determination of vacuum ultraviolet detector response factors by hyphenation with two-dimensional comprehensive gas chromatography with flame ionization detection, *J. Separ. Sci.* 44 (2021) 3849–3859, <https://doi.org/10.1002/jssc.202100459>.
- [163] A. Lelevic, C. Geantet, M. Moreaud, C. Lorentz, V. Souchon, Quantitative analysis of hydrocarbons in gas oils by two-dimensional comprehensive gas chromatography with vacuum ultraviolet detection, *Energy Fuels* 35 (2021) 13766–13775, <https://doi.org/10.1021/acs.energyfuels.1c01910>.
- [164] James X. Mao, Phillip Walsh, Peter Kroll, Kevin A. Schug, Simulation of vacuum ultraviolet absorption spectra: paraffin, isoparaffin, olefin, naphthene, and aromatic hydrocarbon class compounds, *Appl. Spectrosc.* 74 (2019) 72–80, <https://doi.org/10.1177/0003702819875132>.
- [165] L. Ho Manh, V.C.P. Chen, J. Rosenberger, S. Wang, Y. Yang, K.A. Schug, Prediction of vacuum ultraviolet/ultraviolet gas-phase absorption spectra using molecular feature representations and machine learning, *J. Chem. Inf. Model.* 64 (2024) 5547–5556, <https://doi.org/10.1021/acs.jcim.4c00676>.
- [166] A. Lelevic, C. Geantet, M. Moreaud, C. Lorentz, V. Souchon, Quantification of hydrocarbons in gas oils by GC×GC-VUV: Comparison with other techniques, *Energy Fuels* 36 (2022) 10860–10869, <https://doi.org/10.1021/acs.energyfuels.2c01960>.
- [167] E. Lazzari, M. Piparo, C. Mase, L. Levacher, P.-H. Stefanuto, G. Purcaro, J.-F. Focant, P. Giusti, Chemical elucidation of recycled plastic pyrolysis oils by means of GC×GC-PI-TOF-MS and GC-VUV, *J. Anal. Appl. Pyrolysis* 176 (2023) 106224, <https://doi.org/10.1016/j.jaap.2023.106224>.
- [168] M. Beccaria, M. Piparo, Y. Zou, P.-H. Stefanuto, G. Purcaro, A.L. Mendes Siqueira, A. Maniquet, P. Giusti, J.-F. Focant, Analysis of mixed plastic pyrolysis oil by comprehensive two-dimensional gas chromatography coupled with low- and high-resolution time-of-flight mass spectrometry with the support of soft ionization, *Talanta* 252 (2023) 123799, <https://doi.org/10.1016/j.talanta.2022.123799>.
- [169] Y. Zou, P.-H. Stefanuto, M. Maimone, M. Janssen, J.-F. Focant, Unraveling the complex olefin isomer mixture using two-dimensional gas chromatography-photoionization-time of flight mass spectrometry, *J. Chromatogr. A* 1645 (2021) 462103, <https://doi.org/10.1016/j.chroma.2021.462103>.
- [170] A. Giri, M. Coutriade, A. Racad, K. Okuda, J. Dane, R.B. Cody, J.-F. Focant, Molecular characterization of volatiles and petrochemical base oils by photo-ionization GC×GC-TOF-MS, *Anal. Chem.* 89 (2017) 5395–5403, <https://doi.org/10.1021/acs.analchem.7b00124>.
- [171] E. Lazzari, C. Mase, D.C. Dayton, S. Marceau, G. Purcaro, J.-F. Focant, M. Piparo, P. Giusti, Exploring molecular composition of upgraded pyrolysis bio-oil using GC×GC-(EI/PI)-TOF MS with different column set-ups, *J. Anal. Appl. Pyrolysis* 181 (2024) 106569, <https://doi.org/10.1016/j.jaap.2024.106569>.
- [172] A. Giri, M. Coutriade, A. Racad, P.-H. Stefanuto, K. Okuda, J. Dane, R.B. Cody, J.-F. Focant, Compositional elucidation of heavy petroleum base oil by GC × GC- EI/PI/CI/FI-TOFMS, *J. Mass Spectrom.* 54 (2019) 148–157, <https://doi.org/10.1002/jms.4319>.
- [173] H. Burdová, D. Pilnáj, P. Kurán, Application of low-energy-capable electron ionization with high-resolution mass spectrometer for characterization of pyrolysis oils from plastics, *J. Chromatogr. A* 1711 (2023) 464445, <https://doi.org/10.1016/j.chroma.2023.464445>.
- [174] A. Amirav, A.B. Fialkov, A. Gordin, O. Elkabets, K.J. Margolin Eren, Cold electron ionization (EI) is not a supplementary ion source to standard EI. It is a highly superior replacement ion source, *J. Am. Soc. Mass Spectrom.* 32 (2021) 2631–2635, <https://doi.org/10.1021/jasms.1c00241>.
- [175] J.M. Halket, V.G. Zaikin, Derivatization in mass Spectrometry—5. Specific derivatization of monofunctional compounds, *Eur. J. Mass Spectrom.* 11 (2005) 127–160, <https://doi.org/10.1255/ejms.712>.
- [176] L.H. Sommer, E.W. Pietrusza, F.C. Whitmore, Peroxide-catalyzed addition of trichlorosilane to 1-octene, *J. Am. Chem. Soc.* 69 (1947) 188.
- [177] Y. Nakajima, S. Shimada, Hydrosilylation reaction of olefins: recent advances and perspectives, *RSC Adv.* 5 (2015) 20603–20616.
- [178] J.M. Halket, V.G. Zaikin, Derivatization in mass Spectrometry—1. Silylation, *Eur. J. Mass Spectrom.* 9 (2003) 1–21, <https://doi.org/10.1255/ejms.527>.
- [179] J.H. Tumlinson, R.R. Heath, R.E. Doolittle, Application of chemical ionization mass spectrometry of epoxides to the determination of olefin position in aliphatic chains, *Anal. Chem.* 46 (1974) 1309–1312, <https://doi.org/10.1021/ac60345a028>.
- [180] N.N. Schwartz, J.H. Blumbers, Epoxidations with m-Chloroperbenzoic acid, *J. Org. Chem.* 29 (1964) 1976–1979, <https://doi.org/10.1021/jo01030a078>.
- [181] W.G. Niehaus, R. Ryhage, Determination of double bond positions in polyunsaturated fatty acids by combination gas chromatography-mass spectrometry, *Anal. Chem.* 40 (1968) 1840–1847.
- [182] Y. Xie, P. Chen, L. Hua, K. Hou, Y. Wang, H. Li, Rapid identification and quantification of linear olefin isomers by online ozonolysis-single photon ionization time-of-flight mass spectrometry, *J. Am. Soc. Mass Spectrom.* 27 (2016) 144–152, <https://doi.org/10.1007/s13361-015-1238-3>.
- [183] D.E. Minnikin, P. Abley, F.J. McQuillin, K. Kusamran, K. Maskens, N. Polgar, Location of double bonds in long chain esters by methoxymercuration-demercuration followed by mass spectroscopy, *Lipids* 9 (1974) 135–140.
- [184] R.A. Bernhoft, Mercury toxicity and treatment: a review of the literature, *J. Environ. Public Health* 2012 (2012) 460508, <https://doi.org/10.1155/2012/460508>.
- [185] R.E. Wolff, G. Wolff, J.A. McCloskey, Characterization of unsaturated hydrocarbons by mass spectrometry, *Tetrahedron* 22 (1966) 3093–3101, [https://doi.org/10.1016/S0040-4020\(01\)82288-2](https://doi.org/10.1016/S0040-4020(01)82288-2).
- [186] V. VanRheenen, R.C. Kelly, D.Y. Cha, An improved catalytic OsO₄ oxidation of olefins to cis-1,2-glycols using tertiary amine oxides as the oxidant, *Tetrahedron Lett.* 17 (1976) 1973–1976, [https://doi.org/10.1016/S0040-4039\(00\)78093-2](https://doi.org/10.1016/S0040-4039(00)78093-2).
- [187] J.A. McCloskey, M.J. McClelland, Mass spectra of O-Isopropylidene derivatives of unsaturated fatty esters, *J. Am. Chem. Soc.* 87 (1965) 5090–5093, <https://doi.org/10.1021/ja00950a019>.
- [188] D.A. Carlson, C. Shyan Roan, R.A. Yost, Julio Hector, Dimethyl disulfide derivatives of long chain alkenes, alkadienes, and alkatrienes for gas chromatography/mass spectrometry, *Anal. Chem.* 61 (1989) 1564–1571, <https://doi.org/10.1021/ac00189a019>.
- [189] Marco Vincent, Gianfranco Guglielmetti, Giorgio Cassani, Cristina Tonini, Determination of double-bond position in diunsaturated compounds by mass spectrometry of dimethyl disulfide derivatives, *Anal. Chem.* 59 (1987) 694–699, <https://doi.org/10.1021/ac00132a003>.
- [190] G.W. Francis, K. Veland, Alkylthiolation for the determination of double-bond positions in linear alkenes, *J. Chromatogr. A* 219 (1987) 379–384, [https://doi.org/10.1016/S0021-9673\(00\)80381-7](https://doi.org/10.1016/S0021-9673(00)80381-7).
- [191] T.J. Trinklein, J. Jiang, R.E. Synovec, Profiling olefins in gasoline by bromination using GC×GC-TOFMS followed by discovery-based comparative analysis, *Anal. Chem.* 94 (2022) 9407–9414, <https://doi.org/10.1021/acs.analchem.2c01549>.
- [192] B.A. Parsons, L.C. Marney, W.C. Siegler, J.C. Hoggard, B.W. Wright, R.E. Synovec, Tile-based fisher ratio analysis of comprehensive two-dimensional gas chromatography time-of-flight mass spectrometry (GC × GC-TOFMS) data using a null distribution approach, *Anal. Chem.* 87 (2015) 3812–3819, <https://doi.org/10.1021/ac504472s>.
- [193] W. Hu, J. Niu, R. Bao, C. Dong, H.S. Girmay, C. Xu, Y. Han, Selective characterization of olefins by paternò-büchi reaction with ultrahigh resolution mass spectrometry, *Anal. Chem.* 95 (2023) 15342–15349, <https://doi.org/10.1021/acs.analchem.3c02966>.
- [194] F. Orata, Derivatization reactions and reagents for gas chromatography analysis, *Adv. Gas Chromatograph-Progress Agric., Biomed. Indust. Appl.* 91 (2012).
- [195] S.C. Moldoveanu, V. David, Derivatization methods in GC and GC/MS, in: *Gas Chromatography-Derivatization, Sample Preparation, Application*, 2018. IntechOpen.

- [196] H. Ni, C.S. Hsu, C. Ma, Q. Shi, C. Xu, Separation and characterization of olefin/paraffin in coal tar and petroleum coker oil, *Energy Fuels* 27 (2013) 5069–5075, <https://doi.org/10.1021/ef400470v>.
- [197] D. Jiang, B.G. Sumpter, S. Dai, Olefin adsorption on silica-supported silver salts – A DFT study, *Langmuir* 22 (2006) 5716–5722, <https://doi.org/10.1021/la053415c>.
- [198] A.C.O. Silva, R.A.S. San Gil, C.R. Kaiser, D.A. Azevedo, L.A. D'Avila, Combining NMR and GC-MS to characterize olefin rich fractions of automotive gasolines, *Annals Magnet Reson.* 5 (2006) 11–21.
- [199] F.P. Di Sanzo, Characterization of high boiling fischer-tropsch liquids by liquid and gas chromatography, *Anal. Chem.* 53 (1981) 1911–1914.
- [200] P. Straka, D. Maxa, M. Staš, A novel method for the separation of high-molecular-weight saturates from paraffinic petroleum based samples, *Org. Geochem.* 128 (2019) 63–70, <https://doi.org/10.1016/j.orggeochem.2018.12.002>.
- [201] R.B. Eldridge, Olefin/Paraffin separation technology: a review, *Ind. Eng. Chem. Res.* 32 (1993) 2208–2212.
- [202] O.K. Guha, J. Janak, Charge-transfer complexes of metals in the chromatographic separation of organic compounds, *J. Chromatogr. A* 68 (1972) 325–343.
- [203] T.C. Merkel, R. Blanc, I. Ciobanu, B. Firat, A. Suwarlim, J. Zeid, Silver salt facilitated transport membranes for olefin/paraffin separations: carrier instability and a novel regeneration method, *J. Membr. Sci.* 447 (2013) 177–189, <https://doi.org/10.1016/j.memsci.2013.07.010>.
- [204] J.C. Aponte, J.T. Dillon, Y. Huang, The unique liquid chromatographic properties of group 11 transition metals for the separation of unsaturated organic compounds, *J. Separ. Sci.* 36 (2013) 2563–2570, <https://doi.org/10.1002/jssc.201300457>.
- [205] X. Sun, Y. Song, X. Zhou, Ag-based π -complexation adsorbent for paraffin/olefin separation, *Separ. Sci. Technol.* 58 (2023) 1583–1595, <https://doi.org/10.1080/01496395.2023.2201393>.
- [206] C.E. Rovere, P.T. Crisp, J. Ellis, J. Korth, Chemical class separation of shale oils by low pressure liquid chromatography on thermally-modified adsorbents, *Fuel* 69 (1990) 1099–1104, [https://doi.org/10.1016/0016-2361\(90\)90062-U](https://doi.org/10.1016/0016-2361(90)90062-U).
- [207] S.A. Stout, E.R. Litman, Quantification of synthetic-based drilling mud olefins in crude oil and oiled sediment by liquid column silver nitrate and gas chromatography, *Environ. Forensics* 24 (2023) 256–268, <https://doi.org/10.1080/15275922.2022.2047834>.
- [208] L. Yu, W. Chu, S. Luo, J. Xing, F. Jing, Experimental study of silver-loaded mesoporous silica for the separation of ethylene and ethane, *J. Chem. Eng. Data* 62 (2017) 2562–2569, <https://doi.org/10.1021/acs.jced.7b00069>.
- [209] J.T. Dillon, J.C. Aponte, Y.-J. Tsai, Y. Huang, Thin layer chromatography in the separation of unsaturated organic compounds using silver-thiolate chromatographic material, *J. Chromatogr. A* 1251 (2012) 240–243, <https://doi.org/10.1016/j.chroma.2012.06.042>.
- [210] N.E. Heshka, M. Baltazar, J. Chen, Separation and quantification of olefins and diolefins in cracked petroleum fractions using silver-ion high performance liquid chromatography, *Petrol. Sci. Technol.* 37 (2019) 1808–1816, <https://doi.org/10.1080/10916466.2019.1605378>.
- [211] R. van der Westhuizen, H. Potgieter, N. Prinsloo, A. de Villiers, P. Sandra, Fractionation by liquid chromatography combined with comprehensive two-dimensional gas chromatography–mass spectrometry for analysis of cyclics in oligomerisation products of fischer–tropsch derived light alkenes, *J. Chromatogr. A* 1218 (2011) 3173–3179, <https://doi.org/10.1016/j.chroma.2010.10.009>.
- [212] F. Adam, D. Thiébaud, F. Bertoncini, M. Courtiade, M.-C. Hennion, Supercritical fluid chromatography hyphenated with twin comprehensive two-dimensional gas chromatography for ultimate analysis of middle distillates, *J. Chromatogr. A* 1217 (2010) 1386–1394, <https://doi.org/10.1016/j.chroma.2009.11.092>.
- [213] K. Qian, F.P. Di Sanzo, Detailed analysis of olefins in processed petroleum streams by combined multi-dimensional supercritical fluid chromatography and field ionization time-of-flight mass spectrometry, *Energy Fuels* 30 (2016) 98–103, <https://doi.org/10.1021/acs.energyfuels.5b01921>.
- [214] H. Muller, R.Y. Bakor, T.M. Hoshan, N.A. Alawani, A.S. Al-Hayek, Automated analysis of Petroleum- and plastic-derived fuels by gas chromatography coupled with field ionization mass spectrometry, *Energy Fuels* 38 (2024) 19455–19467, <https://doi.org/10.1021/acs.energyfuels.4c03522>.
- [215] H. Nan, C. Zhang, A. Venkatesh, A.J. Rossini, J.L. Anderson, Argentation gas chromatography revisited: separation of light olefin/paraffin mixtures using silver-based ionic liquid stationary phases, *J. Chromatogr. A* 1523 (2017) 316–320, <https://doi.org/10.1016/j.chroma.2017.06.024>.
- [216] D. Ryoo, J.E. Bara, J.L. Anderson, Polymeric ionic liquids containing copper(I) and copper(II) ions as gas chromatographic stationary phases for olefin separations, *J. Chromatogr. A* 1735 (2024) 465306, <https://doi.org/10.1016/j.chroma.2024.465306>.
- [217] I.D. Souza, H. Nan, M.E.C. Queiroz, J.L. Anderson, Tunable silver-containing stationary phases for multidimensional gas chromatography, *Anal. Chem.* 91 (2019) 4969–4974, <https://doi.org/10.1021/acs.analchem.9b00472>.
- [218] X. Wu, X. Li, L. Xu, W. He, Z. Zhou, W. Liu, F. Zhang, Z. Ren, Application of silver ionic liquid in the separation of olefin and alkane, *J. Chem. Technol. Biotechnol.* 97 (2022) 1207–1214, <https://doi.org/10.1002/jctb.7009>.
- [219] J.-F. Huang, H. Luo, C. Liang, D. Jiang, S. Dai, Advanced liquid membranes based on novel ionic liquids for selective separation of olefin/paraffin via olefin-facilitated transport, *Ind. Eng. Chem. Res.* 47 (2008) 881–888, <https://doi.org/10.1021/ie0707523>.
- [220] Y. Zhang, C. Huang, F. Kong, Y. Wang, Q. Shi, L. Zhang, Selective molecular characterization of olefins in hydrocarbon mixtures by ag+ complexation ESI high-resolution mass spectrometry, *Fuel* 319 (2022) 123760, <https://doi.org/10.1016/j.fuel.2022.123760>.
- [221] Y. Wang, Y. Zhang, Y. Wang, Y. Zhang, C. Xu, Z. Xu, Q. Shi, L. Zhang, C10–C50 olefins in thermal cracking products of heavy petroleum: characterization using ag+ ESI high-resolution mass spectrometry, *Energy Fuels* 39 (2025) 6803–6811, <https://doi.org/10.1021/acs.energyfuels.5c00143>.
- [222] J. Hou, P. Liu, M. Jiang, L. Yu, L. Li, Z. Tang, Olefin/paraffin separation through membranes: from mechanisms to critical materials, *J. Mater. Chem. A Mater.* 7 (2019) 23489–23511.
- [223] H. Dou, B. Jiang, M. Xu, J. Zhou, Y. Sun, L. Zhang, Supported ionic liquid membranes with high carrier efficiency via strong hydrogen-bond basicity for the sustainable and effective olefin/paraffin separation, *Chem. Eng. Sci.* 193 (2019) 27–37, <https://doi.org/10.1016/j.ces.2018.08.060>.
- [224] A.S. Kovvali, H. Chen, K.K. Sirkar, Glycerol-based immobilized liquid membranes for olefin–paraffin separation, *Ind. Eng. Chem. Res.* 41 (2002) 347–356, <https://doi.org/10.1021/ie010100t>.
- [225] K. Nymeijer, T. Visser, R. Assen, M. Wessling, Olefin-selective membranes in gas–liquid membrane contactors for olefin/paraffin separation, *Ind. Eng. Chem. Res.* 43 (2004) 720–727, <https://doi.org/10.1021/ie030594p>.